



**VICTORIA UNIVERSITY**  
MELBOURNE AUSTRALIA

*Impact of compaction method on mechanical characteristics of unbound granular recycled materials*

This is the Accepted version of the following publication

Yaghoubi, Ehsan, Disfani, Mahdi, Arulrajah, Arul and Kodikara, J (2018)  
Impact of compaction method on mechanical characteristics of unbound granular recycled materials. *Road Materials and Pavement Design*, 19 (4). pp. 912-934. ISSN 1468-0629

The publisher's official version can be found at  
<https://www.tandfonline.com/doi/full/10.1080/14680629.2017.1283354>  
Note that access to this version may require subscription.

Downloaded from VU Research Repository <https://vuir.vu.edu.au/38222/>

# **Impact of Compaction Method on Mechanical Characteristics of Unbound Granular Recycled Materials**

EHSAN YAGHOUBI <sup>a</sup>, MAHDI M. DISFANI <sup>b\*</sup>, ARUL ARULRAJAH <sup>a</sup>  
& JAYANTHA KODIKARA <sup>c</sup>

<sup>a</sup> *Department of Civil and Construction Engineering, Swinburne University of Technology, Melbourne, Australia.*

<sup>b</sup> *Department of Infrastructure Engineering, The University of Melbourne, Melbourne, Australia.*

<sup>c</sup> *Department of Civil Engineering, Monash University, Melbourne, Australia.*

*Word count of main text (without tables, figures and ref list): 7,610*

\* Corresponding Author:

Mahdi M DISFANI

Department of Infrastructure Engineering

Melbourne School of Engineering

The University of Melbourne, Parkville, VIC 3010, Australia

Email: mahdi.miri@unimelb.edu.au

Phone: + 61 3 8344 5972

# **Impact of Compaction Method on Mechanical Characteristics of Unbound Granular Recycled Materials**

Laboratory testing methods are constantly being developed to simulate true field conditions in controlled laboratory environment. The aim of laboratory testing methods is to reproduce specimens which accurately replicate field performance in terms of mechanical behavior of pavement materials under applied loads. Compaction is the most common soil stabilization technique in ground improvement and pavement construction works. Among the available laboratory compaction methods, impact method followed by the static method are the most commonly used procedures. Since the nature and approach of these two compaction methods is fundamentally different, an investigation on the effect of using these techniques on the mechanical performance of pavement materials prepared by each of these methods is essential, so as to better understand both these compaction methods. In this regard, two types of recycled Construction and Demolition (C&D) materials suitable for pavement applications, being Crushed Brick (CB) and Recycled Concrete Aggregate (RCA) were selected. Laboratory specimens were prepared using the two above-mentioned procedures. Different aspects of geotechnical characteristics of the specimens, including aggregate breakage, changes in soil-water characteristics, stiffness and resilient characteristics, etc., were investigated. The outcomes of this research indicate that the influence of method of compaction must be considered when interpreting the laboratory test results for field design purposes.

Keywords: Static Compaction, Impact Compaction, Aggregate Breakage, Recycled Material, Unbound Granular Materials, Resilient Modulus

## **Introduction**

Compaction is a soil stabilization technique for increasing the strength characteristics of soils and aggregates and to also reduce their deformation potential. This is achieved by applying mechanical energy to lower voids from the soil matrix. Compaction in the field is achieved using a variety of methods. The four most common techniques for field compaction are: dynamic (e.g. dropping weights), kneading (e.g. applying sheep

foot/rubber-tired rollers), vibration (e.g. vibratory rollers), and static compaction (e.g. smooth wheel rollers) (Browne, 2006). Accordingly, laboratory testing methods have been developed for simulating the field condition in order to prepare test specimens to evaluate the properties of pavement materials.

The current laboratory compaction techniques are used to determine two important pavement and geotechnical design and construction parameters: Optimum Moisture Content (OMC) and Maximum Dry Density (MDD). These two parameters are then used to control field compaction and to achieve certain performance. However, OMC and MDD in the lab are obtained by applying specific compaction energy. Therefore, these parameters can vary depending on the magnitude and nature of compaction energy (Reddy & Jagadish, 1993). Figure 1, as an instance, shows how increasing the energy of compaction results in decrease in OMC and increase in MDD of the same material. In this case, energy of compaction is increased by adding to the number of drops of compaction hammer per layer of the material.

The most widely used laboratory compaction techniques are impact and static compaction (Kouassi, Breyse, Girard, & Poulain, 2000). Normally, impact method is used for field compaction control, and sample preparation. Alternatively, static method is used for sample preparation in research projects using the compaction parameters obtained from impact method.

The standard and modified Proctor tests are the most common impact compaction methods. The standard Proctor test was first developed in the 1930s, but due to technological advancements in heavy rollers, it was often deemed to be unable to represent true field conditions. Accordingly, the modified Proctor compaction technique was developed in the 1940s. In the modified method compaction energy was increased from 594 to 2700 kN-m/m<sup>3</sup> (Das, 2010). While impact compaction involves repeated

dropping of a hammer of specific weight from a determined height for a defined number of blows, in the static compaction approach, pressure is applied at the surface of each layer in the compaction mold and maintained long enough until change in axial displacement reaches zero or until the required density (or void ratio) is achieved.

Field compaction is normally performed using compaction machinery which applies static pressure solely, or together with actions such as vibration and kneading. To simulate this compaction process in the laboratory, the determination of energy input per unit volume of the soil in field and laboratory is essential. This causes two problems in using the impact method. Firstly, the nature of laboratory compaction is different to the static or kneading method implemented in the field. Secondly, the impact compaction method applies a defined energy input; whereas in the field, different types of compaction machinery are used applying different compaction energies to the soil (Reddy & Jagadish, 1993). Therefore, the OMC obtained from impact methods, cannot necessarily be suitable for field compaction. Another drawback of the impact method observed during compaction procedure of granular material is that aggregates escape from underneath the hammer contact surface. On the other hand, in static compaction the main drawback is that the displacement of the aggregates under compaction pressures is limited, since continuous loading and aggregate interlock during static compaction prevent particles from slipping over each other freely. This may cause stress concentration in some parts of the specimen, and accordingly, some higher local density in some parts and larger macro pores in others (Holtz, Kovacs, & Sheahan, 1981). Additionally, in this method, under higher compaction pressures, the void ratio of the samples is decreased to the extent that it gets close to saturation condition. At this stage not only air, but also water is forced out of the sample. This is also the case at higher

water contents, even at lower compaction pressures. This may result in lower obtained water content, compared to what is required in the field to achieve the target density.

This paper presents and discusses a suit of experimental results to investigate the influence of compaction method on hydraulic and mechanical characteristics of two types of Construction and Demolition (C&D) materials commonly used in pavement applications, being Crushed Brick (CB) and Recycled Concrete Aggregate (RCA). Insufficient knowledge and uncertainties on field performance of recycled materials through interpretation of laboratory test results remains a prime reason delaying the widespread application of these materials in pavement construction (A. Arulrajah, Piratheepan, Disfani, & Bo, 2013).

### **Previous Studies**

In spite of developing many laboratory compaction procedures, the impact and static methods are the most accepted laboratory compaction procedures. However, the mechanism of these methods differs from the way soil and aggregates are compacted in the field. Field compaction is the result of one or more of the following actions: static force, vibration, kneading, tamping, and impact blows (Browne, 2006). As a result, researchers have investigated laboratory techniques which can better simulate the field compaction, by including actions such as kneading (Kouassi et al., 2000) or utilizing gyratory compactors originally used for compacting bound material (Browne, 2006). However, the difficulties and complexities of applying these compaction techniques is the prime reason that the impact and static methods have remained as most commonly used methods. Static compaction is known to be a faster, simpler and easier method of compaction compared to the impact method (Asmani, Hafez, & Shakri, 2013). Therefore, in recent years, static compaction has been the more common specimen preparation technique used for C&D material (Azam & Cameron, 2013; Azam,

Cameron, & Rahman, 2013).

Conventionally, compaction is known to be influenced by three factors, being water content, soil type, and compaction effort (Das, 2010). Surprisingly, in sample preparation, the effect of the nature of compaction method is ignored with the aim being to prepare specimens with consistent dry density. A pioneering research comparing static and impact compaction procedures was carried out by Reddy and Jagadish (1993), who focused on making the static method more representative of the true field conditions. The OMC and MDD values obtained from this method were believed to correlate well with field compaction operations. Hafez, Asmani, and Nurbaya (2010) chose five different types of soils and compared the OMC and MDD values obtained from static and impact method with field results and suggested that the static method provides a more sensible representation of field conditions compared to the impact method. Asmani, Hafez, and Nurbaya (2011) investigated the uniformity of specimens prepared using the impact and static compaction methods based on the density and water content of the top and bottom layers of the specimens. They concluded that impact compaction results in non-uniformity across the specimen height. Asmani et al. (2011) supported their conclusion by using X-ray tests on specimens prepared by static and impact compaction, and concluded that the static procedure resulted in more uniform specimens.

A common approach in using static compaction for pavement material specimen preparation is to obtain OMC and MDD from the impact method, and use these values to compact samples. Crispim et al. (2011) prepared specimens with insignificant density difference (1 to 3 %) using static and impact method and conducted Unconfined Compressive Strength (UCS) tests on the specimens. In spite of achieving almost the same densities, UCS values for statically prepared specimens were found to be 20%

lower for clay of high plasticity and 37% higher for clayey sand. In order to conduct more investigations, Crispim et al. (2011) took photomicrographs of the specimens prepared by the two methods and observed that unlike specimens prepared with impact method, statically prepared specimens presented a fairly uniform distribution of porosity. They suggested that this may be the reason for different mechanical strength in the specimens.

In materials with a significant coarse fraction, the structure of aggregates changes during compaction. This alteration of particle size is due to breakage of the particles, especially the coarse fraction of a blend. Studies show that aggregate breakage changes the hydraulic states of soil, and accordingly affects the unsaturated behavior of soils (Zhang & Buscarnera, 2015). Since pavement material tends to be unsaturated during their service life, these changes in unsaturated behavior of compacted material (in subgrade, sub-base or base) should be taken into account. The capillary potential of soil results in an inter-particle normal force that contributes to the stiffness of soil against external loading (Alonso, Gens, & Josa, 1990). This inter-particle pull is matric suction (hereafter referred to as suction) and is increased by reduction in size of soil pores (i.e. reduction in equivalent radius of a capillary tube). Compaction alters the Particle Size Distribution (PSD) of a blend due to breakage resulting in larger values of suction (Zhang & Buscarnera, 2015). This is because breakage causes increase in the percentage of the smaller sized particles, resulting in smaller pore sizes, and accordingly, higher values of suction at a specific degree of saturation. Soil Water Characteristic Curve (SWCC) relates the moisture content of soil to its suction. PSD affects SWCC, since it influences formation of the network of capillary pores inside a block of soil.

Compared to cohesive soils, suction is rather small in unbound granular pavement materials due to larger size of pores in their structure. As a result, few studies have been done on the unsaturated behavior of the unbound granular materials compared to many studies on unsaturated behavior of fine soils. However, there are some recent studies on the influence of suction on unbound granular materials mechanical performance with the mutual agreement that the effect of suction forces cannot be ignored (Azam & Cameron, 2013; Azam et al., 2013; Ba, Nokkaew, Fall, & Tinjum, 2013; Cameron, 2014; Rahardjo, Satyanaga, Leong, & Wang, 2013; Yang, Lin, Kung, & Huang, 2008). Nevertheless, in these research works effect of compaction method and the resulting alteration in PSD has not been considered. To the best of authors' knowledge, this is the first time that changes in soil-water characteristics of unbound granular materials due to changes in the PSD as a result of compaction is investigated.

The few abovementioned investigations show that the difference in the nature of the impact method of compaction and static method of compaction can result in specimens with different behavior and characteristics. However, this important factor (method of compaction) has normally been ignored in researches conducted on pavement granular materials. Hence, a detailed investigation on the influence of these laboratory compaction procedures on mechanical performance of the specimens prepared using these techniques is required. The primary objective of this research is to propose, for the first time, a testing approach to compare the impact method of compaction with static method of compaction. Further, the two compaction methods are evaluated and compared by considering a series of tests to study the influence of compaction technique on a range of mechanical performance characteristics, including soil-water, stiffness, and resilient characteristics of the laboratory specimens.

## **Materials and Methods**

Two types of C&D materials, being Crushed Brick (CB), and Recycled Concrete Aggregate (RCA), suitable for pavement subbase applications were used in this research (Arul Arulrajah, Disfani, Horpibulsuk, Suksiripattanapong, & Prongmanee, 2014). The materials were collected from a major recycling facility in Melbourne, Australia. Table 1 presents the geotechnical properties of CB and RCA material used in this research as evaluated in the laboratory. Previous researches such as Arul Arulrajah et al. (2014) and A. Arulrajah et al. (2013), among others show that CB and RCA have physical properties comparable to typical quarry materials. In particular, Los Angeles abrasion value of both CB and RCA is lower than maximum limit of this property for conventional unbound granular materials used in pavements (Arul Arulrajah et al., 2014). As a result, the amount of aggregate breakage during compaction for CB and RCA is expected to be similar to that of typical base/subbase granular materials.

In this research, two compaction procedures were applied for sample preparation: static compaction under several pressures using several constant pressures and impact compaction using modified Proctor effort (ASTM D1557-12 (2012)). To assure maximum consistency, as well as repeatability, prior to compaction, materials were split in three portions of particle size range. Then these three portions being: particles smaller than 2.36 mm, those between 2.36 and 9.5 mm, and those larger than 9.5 mm were mixed in specific percentages to reconstitute samples with consistent PSD. In order to verify this, 3 trial samples were prepared by mixing the abovementioned portions and were then re-sieved. Then the standard deviation of the %passing each sieve size was calculated for the three obtained PSDs. Standard deviations of between 0.3 and 1.8% for CB and 0.2 and 1.5% for RCA shows negligible difference in PSD of the samples prepared using the abovementioned procedure. For checking the

repeatability, three CB samples were prepared using the control sieves and wetted to OMC of CB. These were then separately compacted under static pressure of 4000 kPa for comparing their post-compaction dry densities. Obtained dry densities were 1845, 1851, and 1849 kg/m<sup>3</sup>. Since the PSDs and dry densities obtained are very close, and testing procedure is done using automatic/programmable equipment with high precision and control over testing procedure, test results are expected to be repeatable.

Experimental plans are explained in the following sections. In this research, aside from recognized pavement material tests, a testing procedure is proposed to relate impact and static methods of compaction.

### ***Determination of Dry Densities***

In both compaction procedures, molds with diameter of 105 mm and height of 115.5 mm were used and materials were compacted in five layers. The samples were compacted with OMC obtained from modified Proctor method. In static method, targeted pressure was constantly applied on the sample until no further or negligible displacement was observed. Similar to the impact method, in the static procedure, drainage was allowed from the top of the mold. This resulted in reduction in the final moisture content of the specimens prepared under higher compaction pressures or those with the moisture content greater than OMC. Attention was paid to place the same amount of material in the mold for each layer, so that the only variables were the compaction effort and compaction method. Care was taken to avoid segregation while placing the loose material inside the mold. Static compaction was done using a Universal Testing Machine (UTM-100) capable of applying 130 kN of compression axial load. Impact compaction was done using an automatic Proctor compactor set to modified mode.

### ***Proposed Constrained Modulus Testing Approach***

A procedure similar to ASTM D2435-11 (2011), with slight modifications, was used to generate the compression curves of void ratio-vertical stress for specimens prepared following an adaptation of modified Proctor compaction method. The objective of this proposed procedure was to determine the yield stress of the specimens prepared by modified Proctor method by generating the compression curves under several stress levels and applying the Casagrande (1936) method for determination of pre-consolidation stress. Sample preparation was done using molds with diameter of 105 mm and height of 115.5 mm. The compaction procedures (static and impact) mentioned in the previous section were followed; however, in order to maintain the minimum specimen diameter-to-height ratio (according to ASTM D2435-11), samples were compacted in 2 layers, each with a final thickness of approximately 21 mm, following an adaptation of modified Proctor method. Loading was applied using a UTM-100 machine with capacity of 130 kN of compression axial loading. Figure 2 shows a schematic of the constrained modulus test set-up. Two-way drainage was provided for the samples according to ASTM D2435-11. Test data was collected using a data logger for both load and deformation measurements. The compacted samples were subjected to incrementally applied controlled-stress loading. The standard loading schedule consisted of a load increment ratio of 2, starting from 25 kPa, i.e., 25, 50, 100, 200 and finally, 12800 kPa. Each test specimen was kept under each constant loading stage until no or very minor deformation was recorded.

### ***Stiffness and Resilient Characteristics Testing and Calculations***

Sample preparation for stiffness and resilient characteristics testing was done using a split compaction mold with the diameter of 100 mm and height of 202 mm. Specimens

prepared with impact method were compacted in 8 layers, following the procedure described in ASTM-D1557 (2012). For the top layers a collar was used to make sure aggregates remain inside the mold during compaction. Statically prepared specimens were compacted with the similar procedure, but under static compression instead of drops of hammer. Specimens were aimed to have similar densities in order to investigate the influence of method of compaction.

Resilient characteristics of the compacted samples were determined using Repeated Load Triaxial (RLT) tests. RLT test is meant to simulate the pavement layer's condition under repeated traffic loads. For conducting RLT tests, a haversine-shaped loading pulse with 0.1 s loading period and 0.9 s resting period was applied (AASHTO-T307, 2007). A triaxial cell was used with the universal testing machine to carry out the RLT tests. During the tests, specimens were protected from moisture change using a latex membrane. Resilient modulus ( $M_R$ ) is the ratio of a repeated axial stress ( $p_{rep}$ ) to the recoverable axial strain ( $\epsilon_r$ ) caused by the repeated load (Equation 1)

$$M_R = \frac{p_{rep}}{\epsilon_r} = \frac{p_{max} - p_{con}}{\epsilon_r} \quad (1)$$

Where,  $p_{max}$  is the maximum applied vertical stress, and  $p_{con}$  is the contact stress which is the vertical stress applied on the RLT specimen in order to keep the contact between the loading cap and the specimen.

Stiffness characteristics of the compacted samples were determined using Unconfined Compressive Strength (UCS) test. Since RLT test is a non-destructive test, same specimens were used for UCS tests. Conventionally, in UCS test, only the ultimate strength is measured. In this research however, the obtained results were used for determination of other stiffness characteristics of the specimens, being Young's modulus ( $E$ ) and secant modulus ( $E_{50}$ ).  $E$  is the ratio of stress to strain on the  $\sigma$ -strain curve at the elastic zone where the strains are recoverable.  $E_{50}$  is the slope of the line

drawn from the origin to stress that equals half of the UCS peak value on the stress-strain curve. These parameters are presented in Figure 3.

Lateral displacement was also measured to determine Poisson's ratio ( $\nu$ ) and to calculate constrained modulus (oedometric modulus ( $E_{oed}$ )). For this purpose, three LVDTs were installed laterally pointing at the mid-height of the specimen forming 120-degree angles. Poisson's ratio controls the extent to which a sample can be compressed (Thom, 2008). It is defined as the ratio of lateral strain to axial strain under axial loading in the elastic zone of the axial stress-strain curve (Equation 2).

$$\nu = \frac{\varepsilon_l}{\varepsilon_a} \quad (2)$$

Where,  $\varepsilon_l$  is the lateral strain and  $\varepsilon_a$  is the axial strain. Lateral strain values used to calculate the Poisson's ratio were obtained using the average values measured by the 3 lateral LVDTs. Poisson's ratio relates the Young's modulus to constrained modulus ( $E_{oed}$ ). According to Hooke's law  $E_{oed}$  can be obtained using Equation 3:

$$E_{oed} = \frac{(1-\nu)E}{(1-2\nu)(1+\nu)} \quad (3)$$

Where,  $E$  is the Young's modulus, and  $\nu$  is the Poisson's ratio. Values of  $E_{oed}$  obtained from Equation 3 and those obtained from outcomes of the proposed constrained modulus approach are compared in the next section.

## **Results and Discussion**

### ***Yield Stress of Compacted Samples***

The proposed constrained modulus testing approach aimed to determine yield stress of a specimen compacted through the modified Proctor method as the maximum stress that the specimen has experienced in the past. The obtained yield stress was then applied to compact a sample of the same material with the same moisture content, but using static

method. The aim was to investigate whether applying the obtained yield stress using static method would result in a specimen with the MDD of modified Proctor procedure.

To verify the reliability of the above-mentioned approach, three samples were compacted under specific pressures of 2500 kPa, 3000 kPa and 4000 kPa. These pressures were obviously the maximum stress the samples had experienced. In the next step the yield stress of these specimens was estimated using void ratio-pressure curves obtained from the constrained modulus testing approach. Figure 4 shows the void ratio - pressure curves obtained by conducting the proposed testing procedure on the compacted specimens.

Following the Casagrande (1936) method, the compression curves for CB and RCA presented in Figure 4 were analyzed to obtain the yield stress values presented in Table 2. The table also shows the dry densities, as well as the percentage of difference between the compaction pressure and the calculated yield stress.

Results presented in Table 2 show that for the statically compacted samples, the yield stresses obtained are about 40% greater than the maximum pressure applied during compaction. Figure 4 also shows the compression curves for CB and RCA samples compacted using modified Proctor method. Using the Casagrande (1936) method and the  $e$ - $\log p$  curves corresponding to impact compaction presented in Figure 4, the yield stresses for these specimens were determined to be 3140 kPa and 3374 kPa for CB and RCA, respectively. Results presented in Table 2, suggest that the obtained yield stresses are about 40% greater than the maximum pressure experienced by specimens. As an example, RCA sample compacted under 2500 kPa static pressure, resulted in a yield pressure of 3485 kPa (39.4% greater than 2500 kPa) following a one-dimensional compression and Casagrande (1936) procedure. Therefore, it is expected that the maximum equivalent static pressure that CB and RCA specimens, compacted

with modified Proctor compactor, experienced was 2243 kPa and 2410 kPa, respectively. This is because yield pressures of 3140 kPa (40% greater than 2243 kPa) and 3374 kPa (40% greater than 2410 kPa) were obtained from Figure 4. Accordingly, it is expected that static pressures of 2243 kPa and 2410 kPa result in the same dry density as MDD of modified Proctor compaction for CB and RCA, respectively. However, this conclusion is not supported by the experimental results. Static compaction of CB samples under 2250 kPa and RCA under 2400 kPa pressures, results in dry densities less than 90% of their corresponding modified Proctor MDD. This suggests that the method of compaction impacts the mechanical properties of the compacted materials. Furthermore, the proposed procedure cannot predict the static pressure required for preparing a specimen with a dry density identical to MDD of modified Proctor method. In order to develop a better understanding, possible reasons such as differences in gradation curves caused by aggregate breakage during the compaction and consequent changes in suction forces were investigated. Then, stiffness and resilient characteristics of specimens with the same dry density, but prepared using different compaction methods were compared.

### ***Constrained Modulus of the Compacted Samples***

Constrained modulus or oedometeric modulus ( $E_{\text{oed}}$ ) is a parameter obtained from oedometer test. It is defined as the slope of stress-strain curve in geostatic condition (Feeser & Bruckmann, 1995) and is one of the input parameters for describing soil stiffness when the lateral strain is zero. Figure 5 shows the strain versus stress curves obtained from the incremental loading approach for samples compacted by the modified Proctor method and also under static pressures of 2500 and 4000 kPa.

It is apparent from Figure 5 that with changing stress level there is a stronger change in  $E_{\text{oed}}$  of modified Proctor specimen compared to those compacted under static

pressure. In contrast to higher density of modified Proctor (impact) specimen, its  $E_{oed}$  is significantly lower at lower stress intervals, but gradually increases and becomes greater at higher stress intervals (3200 to 6400 kPa and 6400 to 12800 kPa). Same pattern exists for both CB and RCA. This can be related to the different packing and structures developed in the specimens during static and impact compaction. Static specimens tend to have honeycomb structures in their body due to limited freedom of particle displacement during static loading, which is not the case in impact compaction procedure. This causes formation of local particle arches with higher densities that show higher strength against static loading (i.e., oedometer loading), even though this type of structure tends to collapse easier under dynamic loads (Holtz et al., 1981). This is further supported by results of stiffness and resilient characteristics tests presented in the following sections. Values of  $E_{oed}$ , are determined and presented in Table 3.

### ***Densities of the Compacted Samples***

Samples compacted under a static pressure equal to yield stress of modified Proctor specimens (obtained from the proposed constrained modulus testing approach) do not achieve the MDD of modified Proctor procedure. Accordingly, a series of static compaction tests under several pressures were conducted in order to determine the pressure that results in the same density as the MDD of modified Proctor compaction. Densities of the samples compacted under several pressures, as well as those compacted using impact method, are presented in Tables 4 and 5, for CB and RCA, respectively.

The obtained densities/void ratios indicate that under the same compaction pressure, CB samples reach a higher density compared to RCA samples, as is the case in impact compaction. Tables 4 and 5 also show the percentage of MDD of samples compacted under different static pressures to modified Proctor MDD. Changes in relative densities by increasing the compaction pressure from 3000 kPa to 12000 kPa

appear to be uniform for RCA (i.e. a 2% increase at each stress level). This change for CB specimens increases up to 3% at lower pressure levels (3000, 4000 and 6000 kPa) and increases up to 1% increase at higher pressure levels (8000, 10000, 12000 kPa).

Another observation is that with an increasing static compaction pressure, there is a decrease in the post-compaction moisture content of the statically prepared CB specimens. This occurs in the CB specimens that reach a degree of saturation of about 80% or more if they are wetted to the OMC of the modified Proctor method and compacted under static pressure (i.e. 6000 kPa and higher pressures). Under compaction pressure, the aggregates that are non-compressible cannot move; therefore, as the void ratio decreases, not only air, but also water is forced out of the sample. This results in a lower obtained water content in CB specimens, after static compaction, as the compaction pressure increases. However, this is not the case for RCA specimens. This can be attributed to the existence of cement particles in RCA blends that increases the water absorption, as well as existence of fused particles in CB blends that tend to absorb less water. This can clearly be seen by observing the surfaces of CB and RCA particles using micrographs provided in the following sections. Interestingly water absorption of RCA has been reported to be 10% greater than that of CB (A. Arulrajah et al., 2013).

### ***Aggregate Breakage during Compaction***

Sieve analysis was conducted on CB and RCA samples before and after compaction. Figure 6 illustrates the changes in gradation curves before and after applying different compaction pressures, as well as impact compaction. The gradation curves show that aggregate breakage occurs even under lower compaction pressures, i.e., 3000 or 4000 kPa. Figure 6 also shows that PSD of post compaction static specimens under 12000 kPa pressure almost coincides with that of modified Proctor specimens with slight differences

Breakage results in changes in gradation curves and consequently pore network of material. Tables 6 and 7 show changes in gradation parameters, such as  $C_u$  and mean aggregate size ( $D_{50}$ ), before and after compaction for CB and RCA, respectively.

As evident from Tables 6 and 7, the extent of breakage is different under different static pressure levels. Even though, it can be seen from Figure 6 that difference in fine contents, before and after compaction, is not significant. Breakage due to compaction turns gravel particles into sand particles, but it doesn't increase the percentage of particles smaller than  $75 \mu\text{m}$ . Extent of breakage also slightly differs between specimens prepared by static (under 12000 kPa pressure) and impact methods. These differences may be one of the reasons responsible for the different characteristics of samples compacted with different compaction methods.

### ***Changes in Soil Water Characteristics***

Since determination of SWCC in the laboratory or field is challenging and often expensive, predictive models such as Arya and Paris (1981), Aubertin, Mbonimpa, Bussière, and Chapuis (2003), and Likos and Jaafar (2013), among others, are developed to estimate the SWCC using basic geotechnical properties of a material. In order to investigate the effect of type of compaction and the resulted breakage on SWCC, predictive model of Aubertin et al. (2003) was implemented using the PSD of post-compaction material. This model was selected since its input data was available for this research program. Aubertin et al. (2003) model predicts SWCC of materials using the basic and easy-to-obtain geotechnical properties. This model is applicable for both fine grained and granular materials. In case of granular materials, the model requires void ratio,  $D_{10}$ ,  $D_{60}$  and  $C_u$ . These parameters were presented in Tables 6 and 7 for CB and RCA, respectively. Then the link between degree of saturation and suction (SWCC) is obtained through Equations 4 to 6:

$$S_r = S_c + S_a^*(1 - S_c) \quad (4)$$

Where:  $S_c$  is a function of equivalent capillary rise ( $h_{co}$ ), coefficient of uniformity ( $C_u$ ), and suction ( $\psi$ ), and  $S_a^*$  is a function of adhesion coefficient ( $a_c = 0.01$  for granular materials), void ratio ( $e$ ), residual suction ( $\psi_r$ ), suction in complete dryness ( $\psi_0 \approx 10^6$  kPa),  $\psi$  and  $h_{co}$ . Values of  $h_{co}$  and  $\psi_r$  for granular materials are obtained from Equations 5 and 6, respectively.

$$h_{co} = \frac{0.75}{eD_{10}(1.17 \log(C_u)+1)} \quad (5)$$

$$\psi_r = 0.86h_{co}^{1.2} \quad (6)$$

Figure 7 shows the SWCCs of the CB and RCA specimens obtained from the Aubertin et al. (2003) model. SWCCs of CB and RCA show that generally, increasing the compaction pressure results in higher values of suction for an equal degree of saturation. This occurs due to formation of smaller pore sizes which is the result of breakage and/or higher compaction energy that generates denser specimens (i.e. smaller pores). Also, generally in both CB and RCA, for a specific degree of saturation, amount of suction in modified Proctor specimens was greater than that of static specimens.

The section of the curves between 90% and 100% saturation is magnified in Figure 7 for a clearer observation of the influence of compaction approach on the SWCC. This section of the curves, close to the fully saturated condition, is used for determination of the Air Entry Value (AEV). AEV is the suction value that must be reached before air is introduced into the soil pores (Fredlund & Xing, 1994). This is the point where desaturation begins and the behavior of the soil should be investigated in the unsaturated context. AEV of CB samples compacted under 3000 kPa, 12000 kPa

pressure and modified Proctor effort were 0.30, 0.46 and 0.48 kPa, respectively. These values for RCA were 0.25, 0.39, and 0.41 kPa, respectively.

Results presented in Tables 4 and 5 show that the pressures from 3000 kPa to 12000 kPa result in relative densities between 91% to 98% for CB and 88% to 98% for RCA, by taking the MDD modified Proctor method as reference. However, relative AEV of the CB specimens prepared using static method were between 62% and 96% by taking AEV of the specimen compacted using modified Proctor method as reference. The relative AEV for RCA specimens were 62% to 95%. This shows that for a relatively small variation in density (about 10%) there is a quite significant change in AEV of specimens (more than 30%). Also, for modified specimens and static specimens compacted under 12000 kPa which are almost identical in density and have very similar PSD curves, AEV was found to be different. This implies that in C&D material, in addition to density (void ratio) and aggregate breakage, different packing structure caused by different compaction methods influences the formation and size of the pores and consequently suction forces. This in fact, contributes to changes in AEV (and generally, changes in suction values) and for studying the influence of compaction on SWCC of soils, as well as the subsequent field behavior under environmental and external loadings, this factor should be taken into account.

Nevertheless, this should be noted that possible errors in the estimation of SWCC due to model uncertainty can occur. This is important in this case where there is not a significant difference between post-compaction PSD of modified specimens and static specimens compacted under 12000 kPa pressure. Hence, further justification of this through validation of the predicted SWCC by experiments is planned for next stage of this research work.

### *Stiffness Characteristics*

UCS test is the most common test for determining the pavement design parameters, due to its simplicity and the fact that it needs minimum laboratory facilities to be carried out (Piratheepan, Gnanendran, & Lo, 2009). Figure 8 illustrates the stress-strain curves obtained from the UCS tests. Generally, RCA specimens show greater UCS compared to CB specimens. The interesting point is that even though specimens of each type of C&D material have the same densities, those prepared by static compaction result in greater UCS peak values. This indicates that the type of compaction influences the stiffness of compacted samples with the same density. This can be related to the fact that each compaction method results in development of different structures in the specimens. In unbound granular materials, packing arrangement which is to a great extent controlled by the PSD influences the mechanical behavior of granular materials (Santamarina & Cho, 2004). Effect of aggregate packing on potential for permanent deformation (Yideti, Birgisson, Jelagin, & Guarin, 2013), resilient behavior (Yideti, Birgisson, Jelagin, & Guarin, 2014) and California bearing ratio (Yideti, Birgisson, & Jelagin, 2014) is approved through theoretical and experimental research and analysis.

In static procedure, compaction energy is uniformly distributed on top of each layer resulting in specimens with more uniform structures. However, limited feasibility of particle displacement and slipping under constant static pressure during compaction causes stress concentration in some parts of the specimens. This results in formation of honeycomb-like structures in the specimens compacted with static method. In this case, even though, the overall density of static specimens is identical to that of impact specimens, local high density and local low density parts form in the body of the static specimens. Figures 9(a) and 9(b) show a schematic of compacted specimen structures

inspired by the simple procedure mentioned in Holtz et al. (1981). In both Figures 9 (a) and 7 (b), 3 particles sizes, each with equal numbers in both frames are drawn and arranged. This means, both soil specimens shown in Figures 9(a) and 9(b) are identical in PSD (i.e., identical density), but different in the arrangement of particles (i.e., different aggregate packing).

As evident from Figure 9(b), in static specimens a denser arch-like skeleton is formed that can show higher strength against static loads in one direction. This type of structure is stable under static loads (Holtz et al., 1981). In this case, due to higher local density around these arch-like structures that carry the majority of the applied load, higher UCS values was expected (Table 8). This is illustrated in Figure 9 by including the potential force chains, in which thickness of the lines represents the magnitude of the force. More uniform distribution of density in Figure 9 (a) results in more particles contributing to distributing the loads and accordingly, thinner chain force lines. Greater force chain means higher aggregate interlock which results in higher strength in the direction of static loading, as is the case for static specimens in UCS testing. Response of impact and static specimens under dynamic loads is reported and discussed in the next section.

Values of  $E$ ,  $E_{50}$  and Poisson's ratio for the compacted samples are presented in Table 8. Using Equation 1 and applying the values of  $E$  and  $\nu$ , values of  $E_{\text{oad}}$  are calculated and presented in Table 8.

Values of  $E_{\text{oad}}$  were earlier calculated using the void ratio versus vertical pressure curves and presented for several stress levels in Table 3. A comparison between the  $E_{\text{oad}}$  of Table 3 and the values presented in Table 8, shows that they are very similar at stress levels of 100 to 200 kPa, and 200 to 400 kPa. Interestingly, these are about the stress levels at which Poisson's ratios were calculated and used in

Equation 1 to calculate the  $E_{oed}$ . This suggests a correlation between the proposed testing approach and the UCS test for determination of the  $E_{oed}$ .

Table 8 also shows the variation of stiffness parameters for specimens compacted by static and impact methods, even though the dry density of the specimens were the same. This observation further illustrates the impact of compaction method on stiffness characteristics of compacted granular C&D specimens.

### ***Resilient Characteristics***

Resilient modulus ( $M_R$ ) is one of the basic stress-strain relationships required for structural analysis and design of pavement layers subjected to moving wheel loads. However, in none of the research works carried out in this area the influence of compaction method on this characteristic of granular pavement materials has been considered. In this research, specimens of CB and RCA were compacted to their corresponding modified Proctor MDD, using static and modified Proctor method and undergone RLT tests in accordance with AASHTO-T307 (2007) procedure. Figures 10 and 11 illustrate the results of resilient modulus tests, respectively on CB and RCA, in form of resilient modulus versus maximum axial stress. The average values of  $M_R$  for CB specimens prepared by static and modified Proctor method were 132.0 MPa and 241.7 MPa, respectively. These values for RCA were respectively, 196.5 MPa and 255.8 MPa. This shows up to about 80% difference in  $M_R$  values obtained for samples compacted using different methods.

It can be observed from Figures 10 and 11 that regardless of type of C&D material, prepared using both compaction methods, greater confinement stress results in higher resilient moduli. Such a behavior was explained by Puppala, Hoyos, and Potturi (2011) to be attributed to increased densification or stiffness of specimens as the confinement increases. However, in this research, specimens have evidently

experienced significantly higher pressure, by more than 10 times, during the compaction procedure compared to changes in confining pressure from 20.7 to 103 kPa. Therefore, minor changes in confining stress cannot densify the specimens further significantly. The increasing  $M_R$  value may also be related to aggregate interlock. Higher confining pressure brings about greater aggregate interlock, resulting in lower strain under the same axial loading. Figures 10 and 11, also, show that for specimens prepared using both compaction methods, as the deviatoric stress increases in each confinement level,  $M_R$  values increase. This may be due to stress hardening, which is a phenomenon that makes the materials stronger with each cycle of deviatoric loading (Puppala et al., 2011). However, as Figures 10 and 11 show, changes in deviatoric stress have much less influence on  $M_R$  values compared to changes in confining stress, both in impact and static specimens. In other words, magnitude of deviator stress is less influential on resilient modulus of the specimens compared to confining stress. This was also observed in results reported in Hicks and Monismith (1971) and Lekarp, Isacsson, and Dawson (2000).

More importantly, as shown in Figures 10 and 11, impact compaction results in specimens with greater resilient moduli for each type of material, compared to specimens compacted under static pressure. Interestingly, UCS values show that static compaction results in specimens with greater UCS peak values (Table 8). This behavior may be related to the structure of the specimens after static or impact compactions. As discussed in the previous section, in static method honeycomb-like structures are formed which show higher strength under static loads, i.e., higher UCS peak values. These structures are known to be meta-stable, i.e., stable under static loads but susceptible under vibration or dynamic loads (Holtz et al., 1981). Static specimens of this research show higher recoverable strain, and accordingly, lower resilient modulus.

This is supported by the fact that these specimens showed lower Young's modulus, i.e. the slope of the stress-strain curve where the soil is acting elastically and the strains are recoverable (Table 8). This means that at a specific stress, lower recoverable strain occurs for specimens prepared by the impact method, compared to those prepared by static method. Evidently, the same repeated axial strain that results in lower recoverable strain leads to higher  $M_R$  values.

In terms of C&D material type, average values of  $M_R$  suggest that generally, for specimens prepared under same compaction method and regime, RCA specimens show greater values of resilient modulus compared to CB specimens. This can be related to the fact that RCA particles have higher roughness compared to CB particles. Aggregates with particles of higher roughness values are known to result in higher resilient modulus (Barksdale & Itani, 1989; Lekarp et al., 2000). Scanning Electron Microscopy (SEM) was used for a better observation of the RCA and CB particles. Examples of micrographs of CB and RCA particles are shown in Figure 12. Images 12(a) and 12(d) are micrographs of CB and RCA particles, respectively, with magnification of 1000X. Images 12(b) and 12(c) are 8000X magnified micrographs of areas with smooth surface and rough surface on a CB particle, respectively. Images 12(e) and 12(f) are 8000X magnified micrographs of a RCA particle's surface, both of which show a rough surface. To ensure the surface is not covered with dust and loose mortar, both CB and RCA particles were washed and dried before SEM tests. Observing micrographs of CB and RCA particles indicated that RCA particles almost entirely have a rough surface, whereas CB particles have areas with both rough and smooth surfaces. Smooth surface in CB is due to existence of fused particles of crushed brick. Rougher surface of the RCA particles is in part related to presence of mortar and finer particles bound to the mortar around RCA granules.

Generally, the above-mentioned resilient behaviors suggest two points. Firstly, specimens with same densities prepared using different compaction methods result in very different resilient characteristics. Secondly, higher stiffness doesn't necessarily result in higher  $M_R$  when specimens are prepared using different methods of compaction. In other words, influence of the compaction method needs to be taken into account when the resilient characteristics of granular material are investigated. This is due to the fact that it affects the applicability of mechanical characteristics obtained in laboratory environment for designing and predicting the performance of pavement material compacted in the field using common field compaction machinery.

## **Conclusion**

In this research, a testing procedure was proposed to generate a link between two types of popular compaction methods, being static method and impact method (modified Proctor). Since the testing approach did not suggest a correlation between these methods, several physical and mechanical characteristics of specimens prepared by static and impact methods were investigated. The following conclusions can be drawn from this research, for specimens prepared with the same density but using different compaction methods:

- (1) At the same dry density, post-compaction PSDs of impact and static specimens were almost identical.
- (2) Based on outcomes of the Aubertin et al. (2003) model, SWCC of the specimens was not affected significantly by type of compaction, once the same density was achieved. However, small changes in density caused significant changes in suction values.

- (3) Stiffness and resilient characteristics of compacted samples are highly influenced by the type of compaction, due to difference in formation of specimens' packing structure during the compaction procedure. When different methods of compaction are applied, higher UCS peak values doesn't necessarily result in higher resilient modulus. Static specimens showed greater UCS peak values, but lower resilient modulus.
- (4) For the same method of compaction, RCA specimens showed greater stiffness and greater resilient modulus, as a result of rougher surface of RCA particles.
- (5) The constrained moduli obtained from the proposed testing procedure, showed correlation with those obtained using UCS results.
- (6) Nature of the compaction procedure plays an important role on the Soil-water, stiffness and resilient characteristics of the prepared specimens. Different methods of compaction develop specimens with different structure during densification, in spite of identical densities. Hence, taking a target dry density for sample preparation and ignoring the method of compaction is a misleading approach, especially when simulation of the field condition is intended in laboratory testing.

### **Acknowledgements**

The authors wish to thank Alex Fraser Group (Australia) for providing the Construction and Demolition aggregates for this research project.

### **References**

AASHTO-T307. (2007). Standard Method of Test for Determining the Resilient Modulus of Soils and Aggregate Materials. Washington, DC: American Association of State Highway and Transportation Officials.

- Alonso, E. E., Gens, A., & Josa, A. (1990). A Constitutive Model for Partially Saturated Soils. *Geotechnique*, 40(3), 405-430.
- Arulrajah, A., Disfani, M. M., Horpibulsuk, S., Suksiripattanapong, C., & Prongmanee, N. (2014). Physical Properties and Shear Strength Responses of Recycled Construction and Demolition Materials in Unbound Pavement Base/Subbase Applications. *Construction and Building Materials*, 58, 245-257.  
doi:<http://dx.doi.org/10.1016/j.conbuildmat.2014.02.025>
- Arulrajah, A., Piratheepan, J., Disfani, M. M., & Bo, M. W. (2013). Geotechnical and Geoenvironmental Properties of Recycled Construction and Demolition Materials in Pavement Subbase Applications. *Journal of Materials in Civil Engineering*, 25(8), 1077-1088. doi:10.1061/(ASCE)MT.1943-5533.0000652
- Arya, L. M., & Paris, J. F. (1981). A Physicoempirical Model to Predict the Soil Moisture Characteristic from Particle-Size Distribution and Bulk Density Data. *Soil Science Society of America Journal*, 45(6), 1023-1030.
- Asmani, D. M. Y., Hafez, M. A., & Nurbaya, S. (2011). Static Laboratory Compaction Method. *Electronic Journal of Geotechnical Engineering*, 16 M, 1583-1593.
- Asmani, D. M. Y., Hafez, M. A., & Shakri, M. S. (2013). Comparison between Static and Dynamic Compaction for California Bearing Ratio (CBR). *Electronic Journal of Geotechnical Engineering*, 18 Y, 5857-5869.
- ASTM-D1557. (2012). Standard Test Methods for Laboratory Compaction Characteristics of Soil Using Modified Effort (56,000 ft-lbf/ft<sup>3</sup> (2,700 kN-m/m<sup>3</sup>)). West Conshohocken, PA: ASTM International.
- ASTM-D2435. (2011). Standard Test Methods for One-Dimensional Consolidation Properties of Soils Using Incremental Loading. West Conshohocken, PA: ASTM International.
- Aubertin, M., Mbonimpa, M., Bussière, B., & Chapuis, R. P. (2003). A Model to Predict the Water Retention Curve from Basic Geotechnical Properties. *Canadian Geotechnical Journal*, 40(6), 1104-1122. doi:10.1139/t03-054
- Azam, A. M., & Cameron, D. A. (2013). Geotechnical Properties of Blends of Recycled Clay Masonry and Recycled Concrete Aggregates in Unbound Pavement Construction. *Journal of Materials in Civil Engineering*, 25(6), 788-798. doi:10.1061/(asce)mt.1943-5533.0000634
- Azam, A. M., Cameron, D. A., & Rahman, M. M. (2013). Model for prediction of resilient modulus incorporating matric suction for recycled unbound granular materials. *Canadian Geotechnical Journal*, 50(11), 1143-1158. doi:10.1139/cgj-2012-0406
- Ba, M., Nokkaew, K., Fall, M., & Tinjum, J. M. (2013). Effect of Matric Suction on Resilient Modulus of Compacted Aggregate Base Courses. *Geotechnical and Geological Engineering*, 31(5), 1497-1510. doi:10.1007/s10706-013-9674-y
- Barksdale, R. D., & Itani, S. Y. (1989). Influence of Aggregate Shape on Base Behavior. *Transportation Research Record*, 1227, 173-182.

- Browne, M. (2006). *Feasibility of Using a Gyrotory Compactor to Determine Compaction Characteristics of Soil*. (Master of Science Thesis), Montana State University, Bozeman, Montana.
- Cameron, D. A. (2014). *Expansive Clays, Collapsing Sands, Unbound Pavement Materials and Unsaturated Soil Theory*. Paper presented at the Proceedings of the 6th International Conference on Unsaturated Soils (UNSAT 2014),. <http://www.scopus.com/inward/record.url?eid=2-s2.0-84901621067&partnerID=40&md5=4ddcadde18aa28b0c81e242735824486>
- Casagrande, A. (1936). *The Determination of the Pre-Consolidation Load and its Practical Significance*. Paper presented at the Proceedings of the International Conference on Soil Mechanics and Foundation Engineering, Harvard University Press, Cambridge, MA.
- Crispim, F. A., de Lima, D. C., Schaefer, C. E. G. R., de Carvalho Silva, C. H., de Carvalho, C. A. B., de Almeida Barbosa, P. S., & Brandão, E. H. (2011). The Influence of Laboratory Compaction Methods on Soil Structure: Mechanical and Micromorphological Analyses. *Soils and Rocks*, 34(1), 91-98.
- Das, B. M. (2010). *Principles of Geotechnical Engineering* (7th ed. ed.). Stamford, CT: Cengage Learning.
- Feeser, V., & Bruckmann, W. (1995). *Data report: Oedometer and Triaxial Tests of Sediment from the Chile Triple Junction*. Paper presented at the Proceedings of the Ocean Drilling Program. Scientific Results.
- Fredlund, D. G., & Xing, A. (1994). Equations for the Soil-Water Characteristic Curve. *Canadian Geotechnical Journal*, 31(4), 521-532.
- Hafez, M. A., Asmani, D. M. Y., & Nurbaya, S. (2010). Comparison between Static and Dynamic Laboratory Compaction Methods. *Electronic Journal of Geotechnical Engineering*, 15, 1641-1650.
- Hicks, R. G., & Monismith, C. L. (1971). Factors Influencing the Resilient Response of Granular Materials. *Highway research record*, 34(345), 15-31.
- Holtz, R. D., Kovacs, W. D., & Sheahan, T. C. (1981). *An Introduction to Geotechnical Engineering* (Second ed.): Pearson Education, Inc.
- Kouassi, P., Breyse, D., Girard, H., & Poulain, D. (2000). A New Technique of Kneading Compaction in the Laboratory. *Geotechnical Testing Journal*, 23(1), 72-82.
- Lekarp, F., Isacsson, U., & Dawson, A. (2000). State of the Art. I: Resilient Response of Unbound Aggregates. *Journal of Transportation Engineering*, 126(1), 66-75.
- Likos, W. J., & Jaafar, R. (2013). Pore-Scale Model for Water Retention and Fluid Partitioning of Partially Saturated Granular Soil. *Journal of Geotechnical and Geoenvironmental Engineering*, 139(5), 724-737.
- Piratheepan, J., Gnanendran, C., & Lo, S. (2009). Characterization of Cementitiously Stabilized Granular Materials for Pavement Design Using Unconfined Compression and IDT Testings with Internal Displacement Measurements. *Journal of Materials in Civil Engineering*, 22(5), 495-505. doi:10.1061/(ASCE)MT.1943-5533.0000051

- Puppala, A. J., Hoyos, L. R., & Potturi, A. K. (2011). Resilient Moduli Response of Moderately Cement-Treated Reclaimed Asphalt Pavement Aggregates. *Journal of Materials in Civil Engineering*, 23(7), 990-998. doi:10.1061/(ASCE)MT.1943-5533.0000268
- Rahardjo, H., Satyanaga, A., Leong, E. C., & Wang, J. Y. (2013). Unsaturated Properties of Recycled Concrete Aggregate and Reclaimed Asphalt Pavement. *Engineering Geology*, 161, 44-54. doi:10.1016/j.enggeo.2013.04.008
- Reddy, B. V. V., & Jagadish, K. S. (1993). The Static Compaction of Soils. *Geotechnique*, 43(2), 337-341.
- Santamarina, J., & Cho, G. (2004). *Soil behaviour: The role of particle shape*. Paper presented at the Advances in geotechnical engineering: The skempton conference.
- Thom, N. (2008). *Principle of Pavement Engineering*. London, UK: Thomas Telford Publishing.
- Yang, S.-R., Lin, H.-D., Kung, J. H., & Huang, W.-H. (2008). Suction-Controlled Laboratory Test on Resilient Modulus of Unsaturated Compacted Subgrade Soils. *Journal of Geotechnical and Geoenvironmental Engineering*, 134(9), 1375-1384.
- Yideti, T. F., Birgisson, B., & Jelagin, D. (2014). Influence of aggregate packing structure on California bearing ratio values of unbound granular materials. *Road Materials and Pavement Design*, 15(1), 102-113.
- Yideti, T. F., Birgisson, B., Jelagin, D., & Guarin, A. (2013). Packing theory-based framework to evaluate permanent deformation of unbound granular materials. *International Journal of Pavement Engineering*, 14(3), 309-320.
- Yideti, T. F., Birgisson, B., Jelagin, D., & Guarin, A. (2014). Packing theory-based framework for evaluating resilient modulus of unbound granular materials. *International Journal of Pavement Engineering*, 15(8), 689-697.
- Zhang, Y. D., & Buscarnera, G. (2015). Prediction of Breakage-Induced Couplings in Unsaturated Granular Soils. *Geotechnique*, 65(2), 135-140. doi:10.1680/geot.14.P.086

**List of Tables:**

Table 1. Geotechnical Properties of Recycled C&D Materials

Table 2. Densities and obtained yield pressures of CB and RCA compacted under specific static pressures

Table 3. Constrained modulus of the compacted samples for different stress levels

Table 4. Results of series of compaction tests on CB

Table 5. Results of series of compaction tests on RCA

Table 6. Changes in gradation parameters before and after compaction for CB

Table 7. Changes in gradation parameters before and after compaction for RCA

Table 8. Stiffness characteristics derived from UCS tests for CB and RCA

## **List of Figures:**

Figure 1. Changes in OMC and MDD due to changes in energy of compaction (Das, 2010)

Figure 2. Schematic of testing equipment and details of the compaction mold

Figure 3. Definition of Young's modulus ( $E$ ) and secant modulus ( $E_{50}$ )

Figure 4. Void ratio versus vertical stress curves for samples compacted using static and modified Proctor methods

Figure 5. Strain versus stress curves obtained from the proposed testing approach for (a) CB and (b) RCA

Figure 6. Changes in gradation curves, before and after the compaction for (a) CB and (b) RCA

Figure 7. SWCC of compacted samples of (a) CB and (b) RCA

Figure 8. Stress versus strain curves obtained from UCS tests

Figure 9. Potential arrangement of particles and chain forces in (a) impact samples and (b) static samples with identical densities

Figure 10. Resilient modulus results for CB

Figure 11. Resilient modulus results for RCA

Figure 12. Micrographs of (a, b and c) CB particles, and (d, e and f) RCA particles

Table 1. Geotechnical Properties of Recycled C&D Materials

Material	D <sub>max</sub> (mm)	Coefficient of Curvature (Cc)	Coefficient of Uniformity (Cu)	Specific Gravity		MDD (kg/m <sup>3</sup> )	OMC (%)
				Coarse Fraction	Fine Fraction		
CB	19	0.9	34.6	2.66	2.61	1990	10.8
RCA	19	0.7	28.8	2.66	2.71	1960	11.0

Table 2. Densities and obtained yield pressures of CB and RCA compacted under specific static pressures

Material	Crushed Brick			Recycled Concrete Aggregate		
	2500	3000	4000	2500	3000	4000
Compaction Pressure (kPa)						
Obtained Dry Density (kg/m <sup>3</sup> )	1772.9	1837.4	1850.2	1661.5	1683.0	1729.0
Obtained Yield Pressure (kPa)	3583	4398	5508	3485	3992	5610
Percentage of difference from compaction pressure (%)	43.3	46.6	37.7	39.4	33.1	40.3

Table 3. Oedometeric modulus of the compacted samples for different stress levels

Stress interval (kPa)	E <sub>oed</sub> for material and compaction types (kPa):					
	Static Under 2500 kPa		Static Under 4000 kPa		Modified Proctor	
	CB	RCA	CB	RCA	CB	RCA
25-50	11629	38280	19661	45650	7575	5981
50-100	18897	50243	22938	39129	11363	9570
100-200	33594	48680	39321	49800	18180	16888
200-400	54973	63222	61167	73040	27270	25520
400-800	100783	105332	100091	121733	36976	45936
800-1600	151175	142605	169385	190539	65122	68561
1600-3200	130746	112730	214829	265600	106420	119314
3200-6400	89172	83914	166189	192633	161600	180141
6400-12800	138217	127696	156587	134326	239079	240188

Table 4. Results of series of compaction tests on CB

Compaction pressure (kPa)	3000	4000	6000	8000	10000	12000	Modified Proctor
Target Moisture Content (%)	10.8	10.8	10.8	10.8	10.8	10.8	10.8
Obtained Moisture Content (%)	10.7	10.7	10.5	10.2	10.0	9.7	10.4
MDD (kg/m <sup>3</sup> )	1817.3	1850.9	1911.2	1924.3	1933.5	1941.3	1989.9
Void ratio	0.447	0.421	0.376	0.367	0.36	0.355	0.322
Percentage of achieved MDD to Modified Proctor MDD (%)	91%	93%	96%	97%	97%	98%	100%

Table 5. Results of series of compaction tests on RCA

Compaction pressure (kPa)	3000	4000	6000	8000	10000	12000	Modified Proctor
Target Moisture Content (%)	11.0	11.0	11.0	11.0	11.0	11.0	11.0
Obtained Moisture Content (%)	11.0	11.0	11.0	11.0	10.9	10.9	10.6
MDD (kg/m <sup>3</sup> )	1733.1	1766.0	1801.3	1840.8	1879.5	1929.7	1959.6
Void ratio	0.552	0.523	0.493	0.461	0.431	0.394	0.373
Percentage of achieved MDD to Modified Proctor MDD (%)	88%	90%	92%	94%	96%	98%	100%

Table 6. Changes in gradation parameters before and after compaction for CB

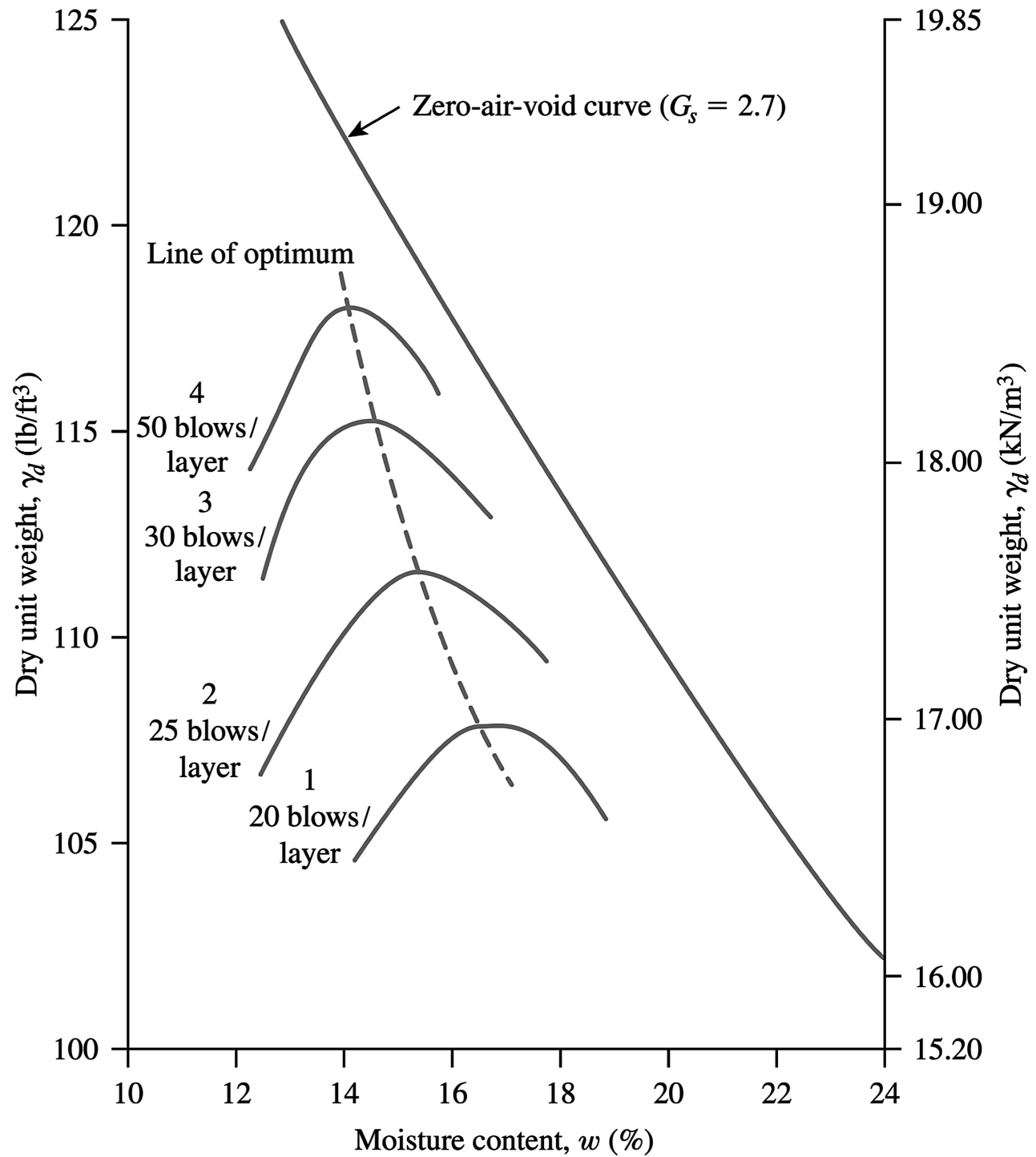
Compaction Type	Before Compaction	Static Compaction under:						Modified Proctor
		3000 kPa	4000 kPa	6000 kPa	8000 kPa	10000 kPa	12000 kPa	
D <sub>10</sub> (mm)	0.20	0.16	0.17	0.15	0.17	0.16	0.15	0.18
D <sub>50</sub> (mm)	4.47	3.87	3.37	3.23	3.15	2.89	2.67	2.65
D <sub>60</sub> (mm)	6.90	6.47	5.60	5.38	5.56	5.17	4.92	4.62
Cu =	34.60	39.90	33.70	35.70	33.50	32.10	32.70	26.30
Change in D <sub>50</sub> (%)	-	13.5%	24.6%	27.8%	29.6%	35.3%	40.3%	40.7%

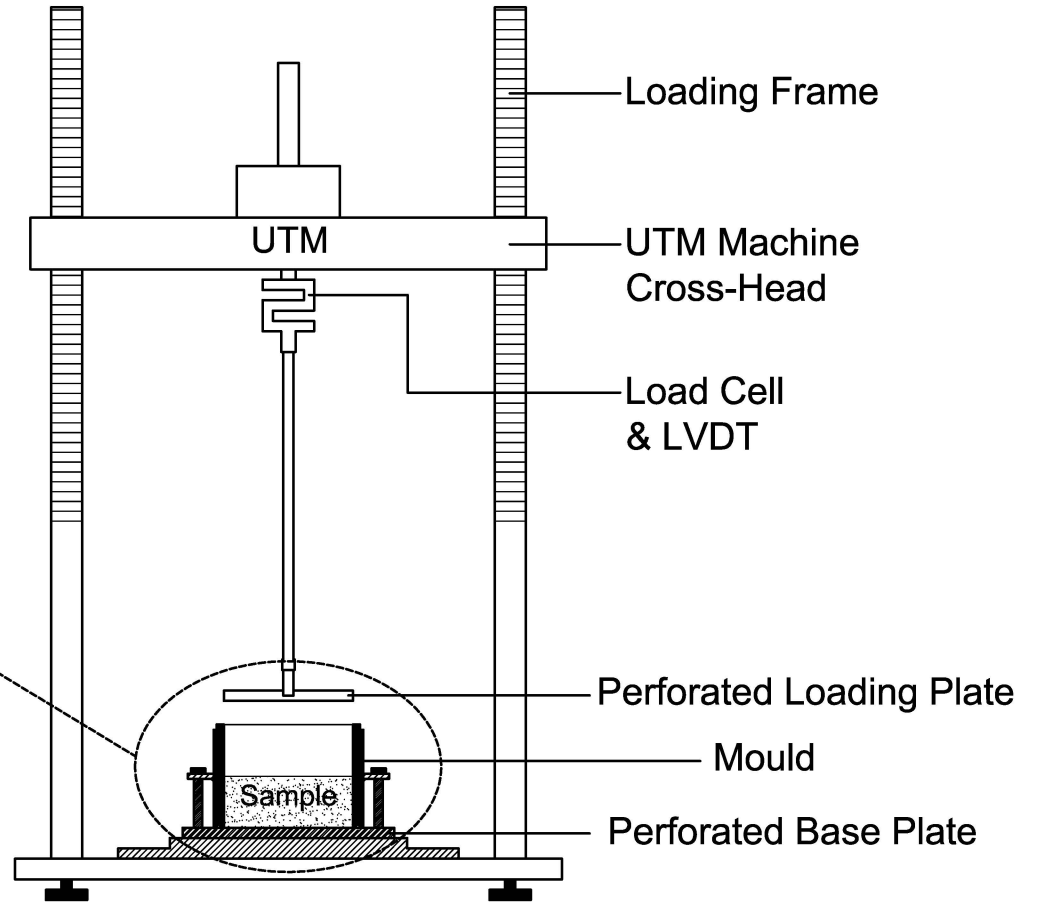
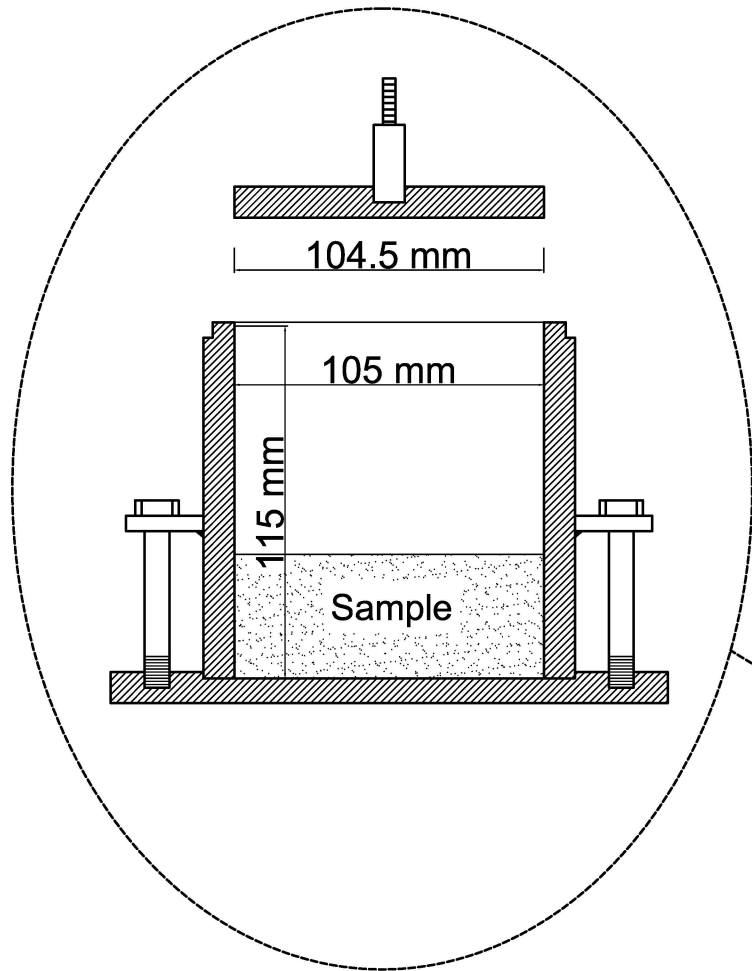
**Table 7. Changes in gradation parameters before and after compaction for RCA**

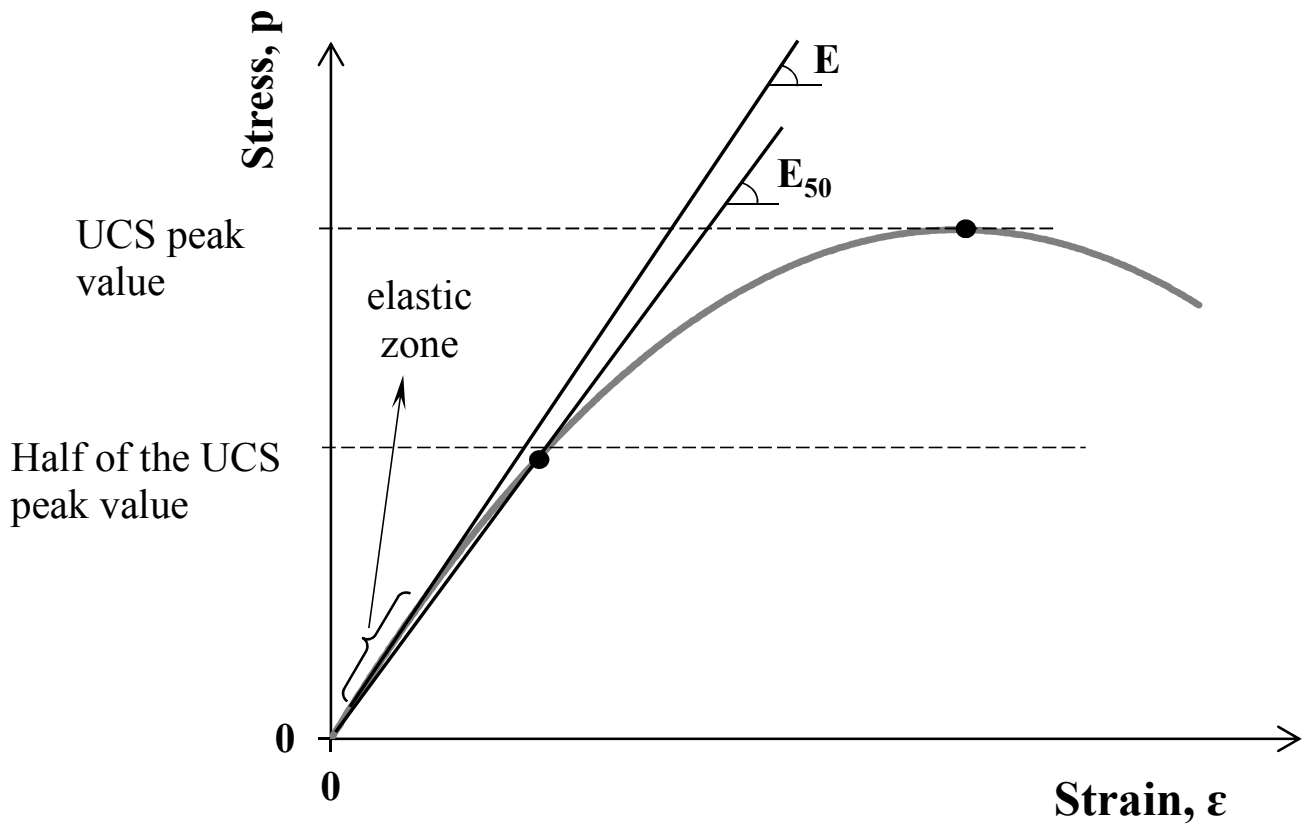
Compaction Type	Before Compaction	Static Compaction under:						Modified Proctor
		3000 kPa	4000 kPa	6000 kPa	8000 kPa	10000 kPa	12000 kPa	
D <sub>10</sub> (mm)	0.25	0.20	0.22	0.22	0.21	0.22	0.20	0.20
D <sub>50</sub> (mm)	5.02	4.15	3.76	3.51	3.45	3.45	3.43	3.36
D <sub>60</sub> (mm)	7.25	6.33	5.84	5.75	5.63	5.60	5.58	5.57
Cu	28.80	31.00	26.80	25.80	27.30	25.10	28.20	28.40
Change in D <sub>50</sub> (%)	-	17.2%	25.1%	30.1%	31.2%	31.3%	31.6%	33.0%

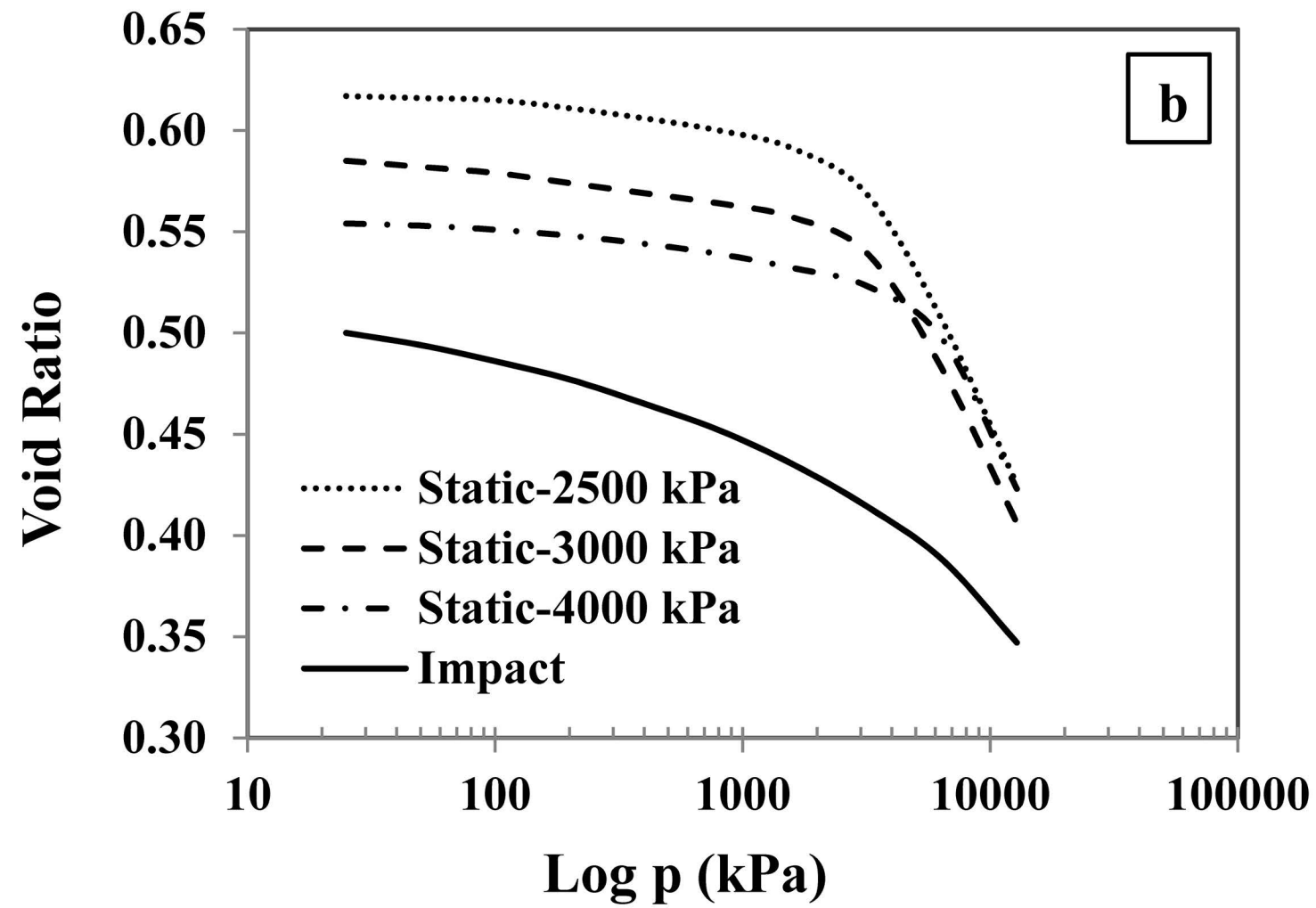
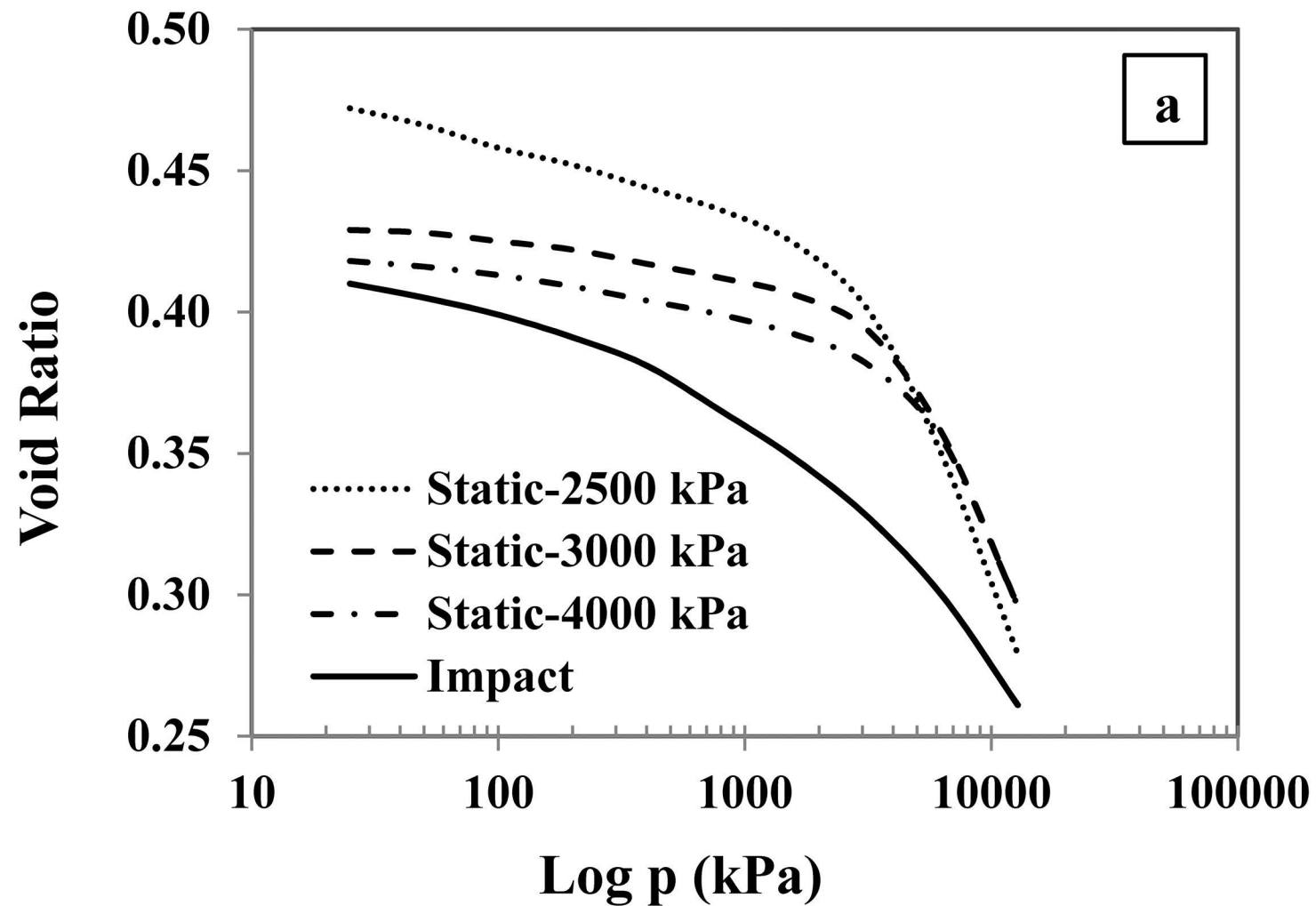
**Table 8. Stiffness characteristics derived from UCS tests for CB and RCA**

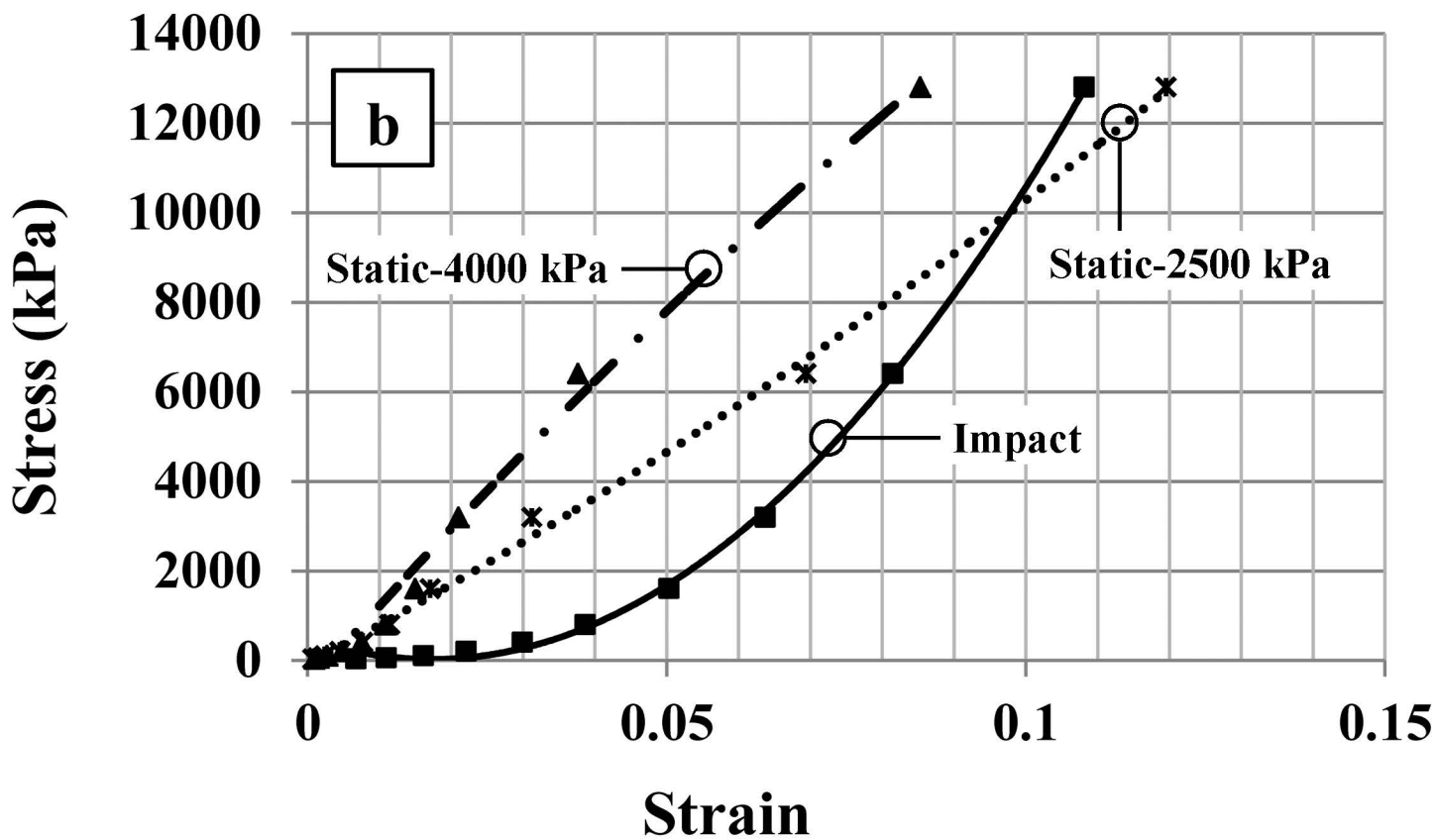
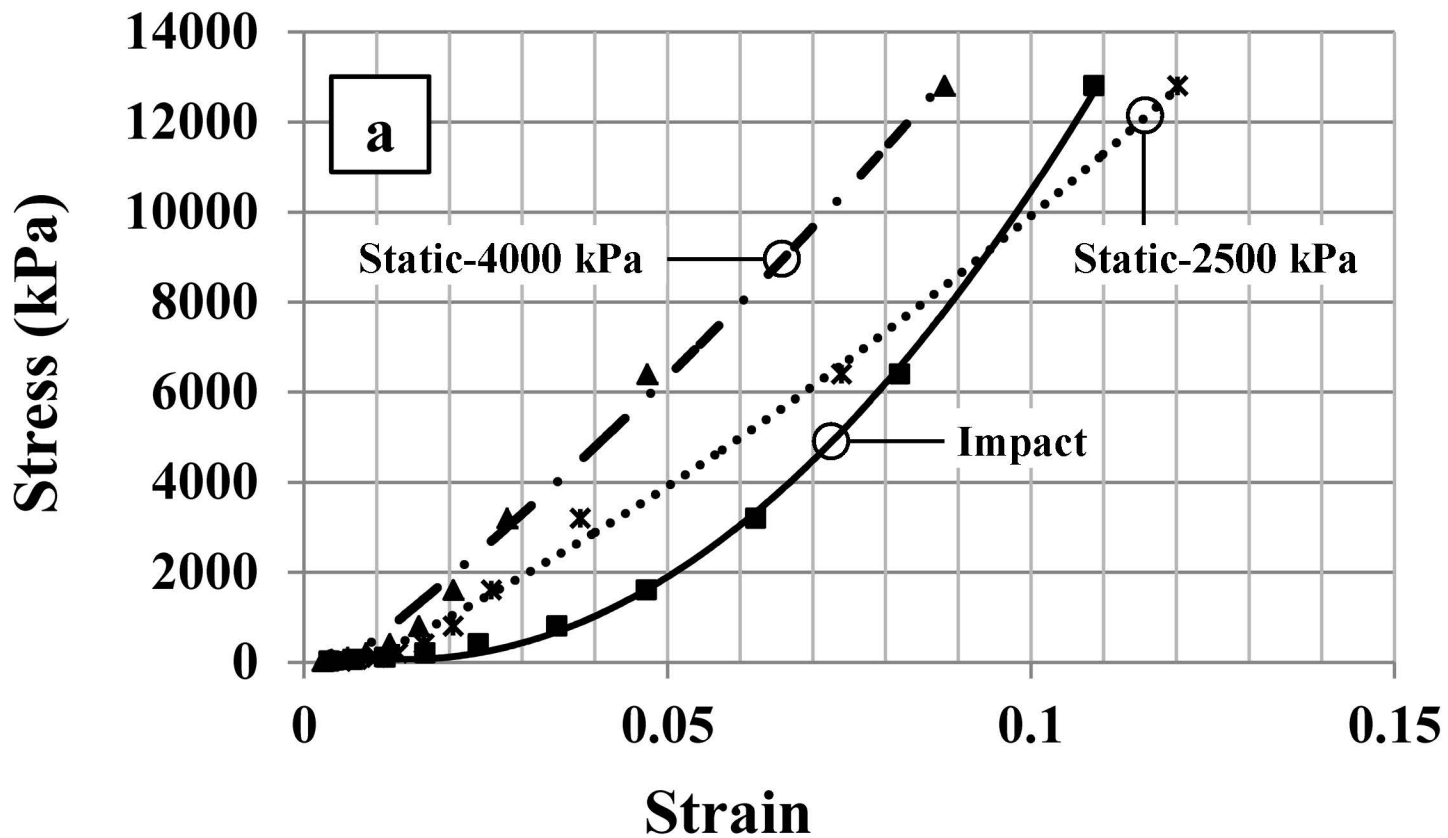
Material	CB		RCA	
	Modified Proctor	Static Under 12000 kPa	Modified Proctor	Static Under 12000 kPa
Specimen Dry Density (kg/m <sup>3</sup> )	1967.3	1952.8	1934.7	1928.1
Specimen Moisture Content (%)	10.3	10	10.4	10.5
UCS Peak Value (kPa)	309.5	358.5	441.0	539.7
E Modulus (kPa)	38866	29401	58147	50621
E <sub>50</sub> Modulus (kPa)	32896	20425	50425	49491
Poisson's Ratio	0.37	0.39	0.26	0.30
E <sub>oed</sub> Modulus (kPa)	8895	6406	17075	13509

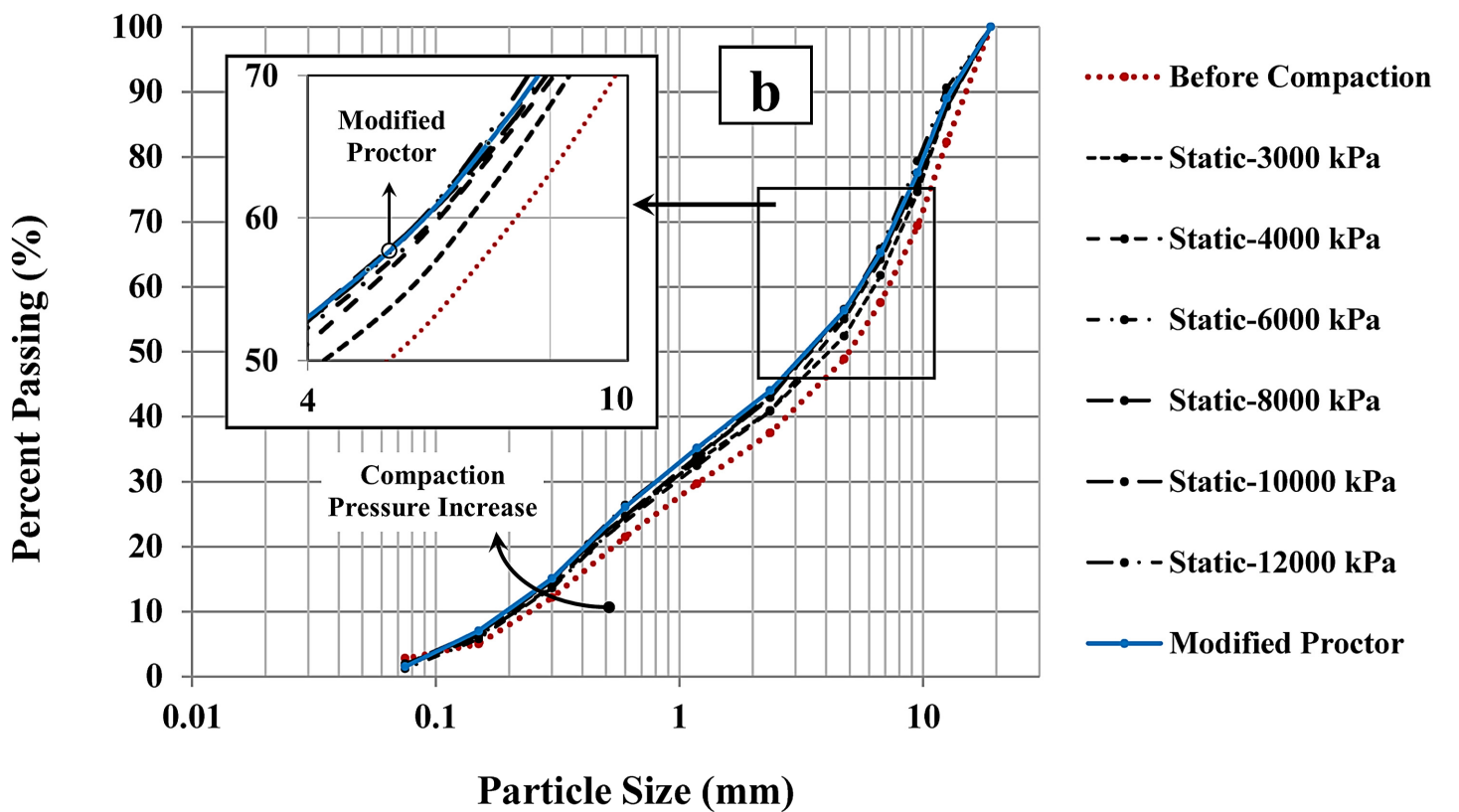
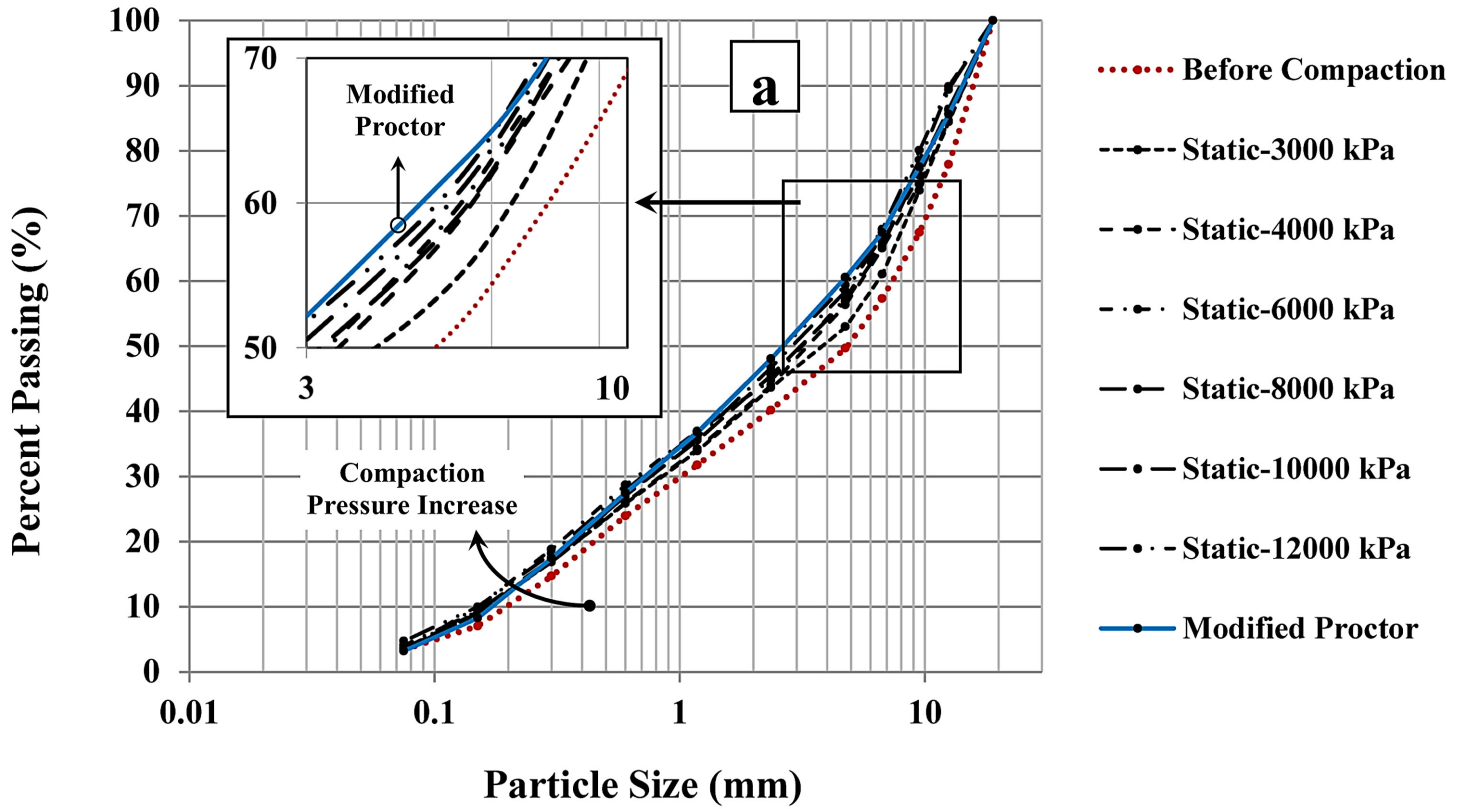


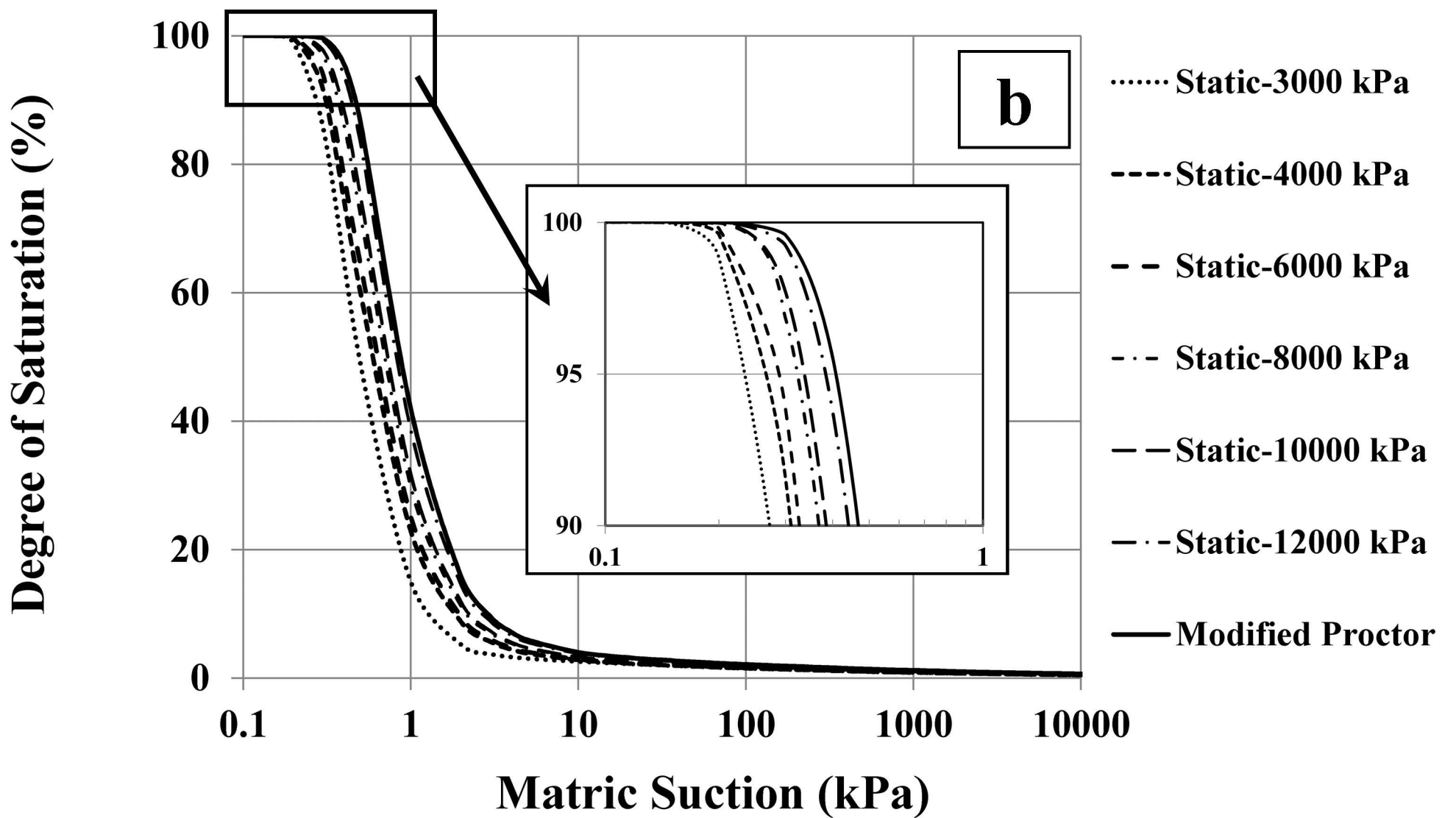
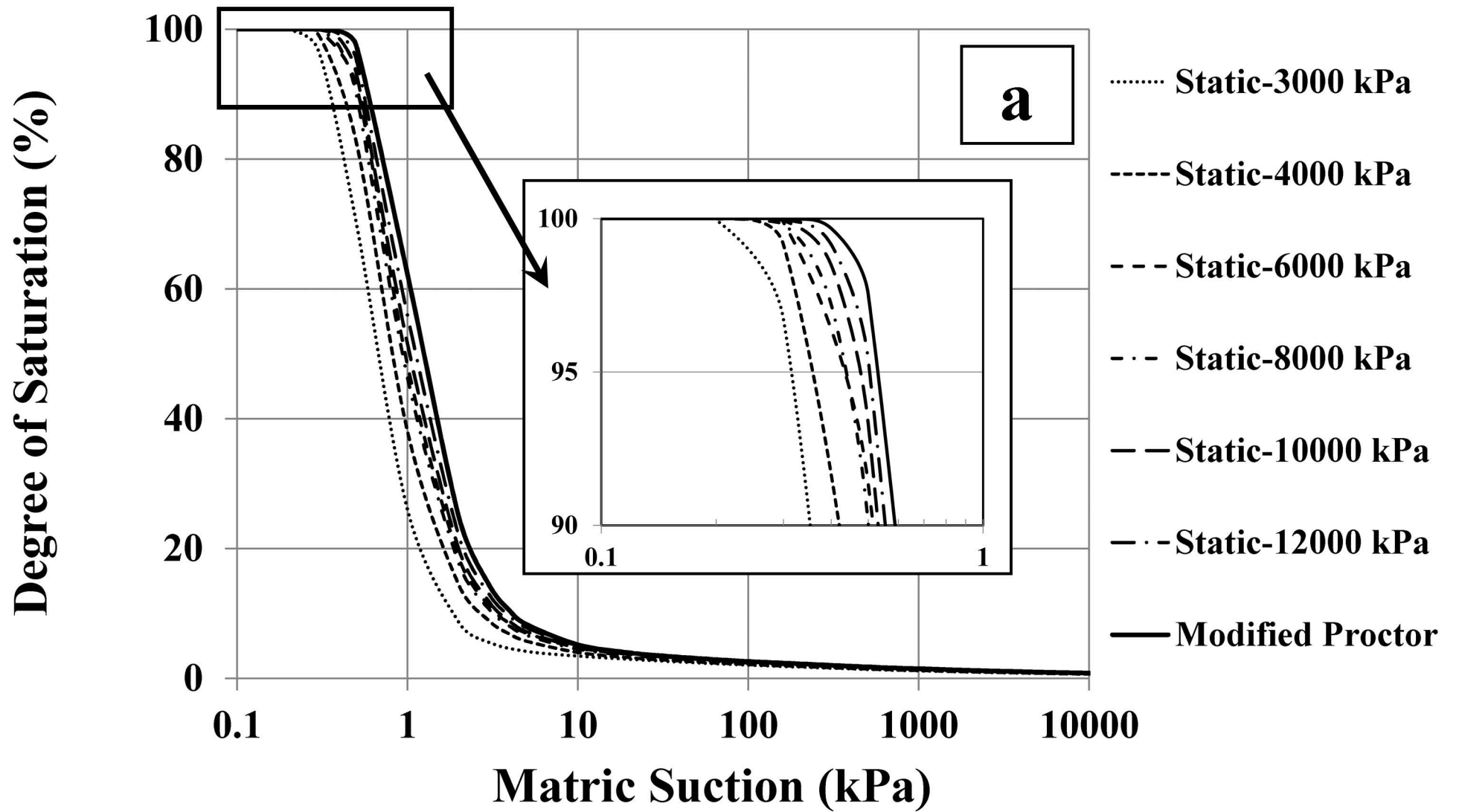


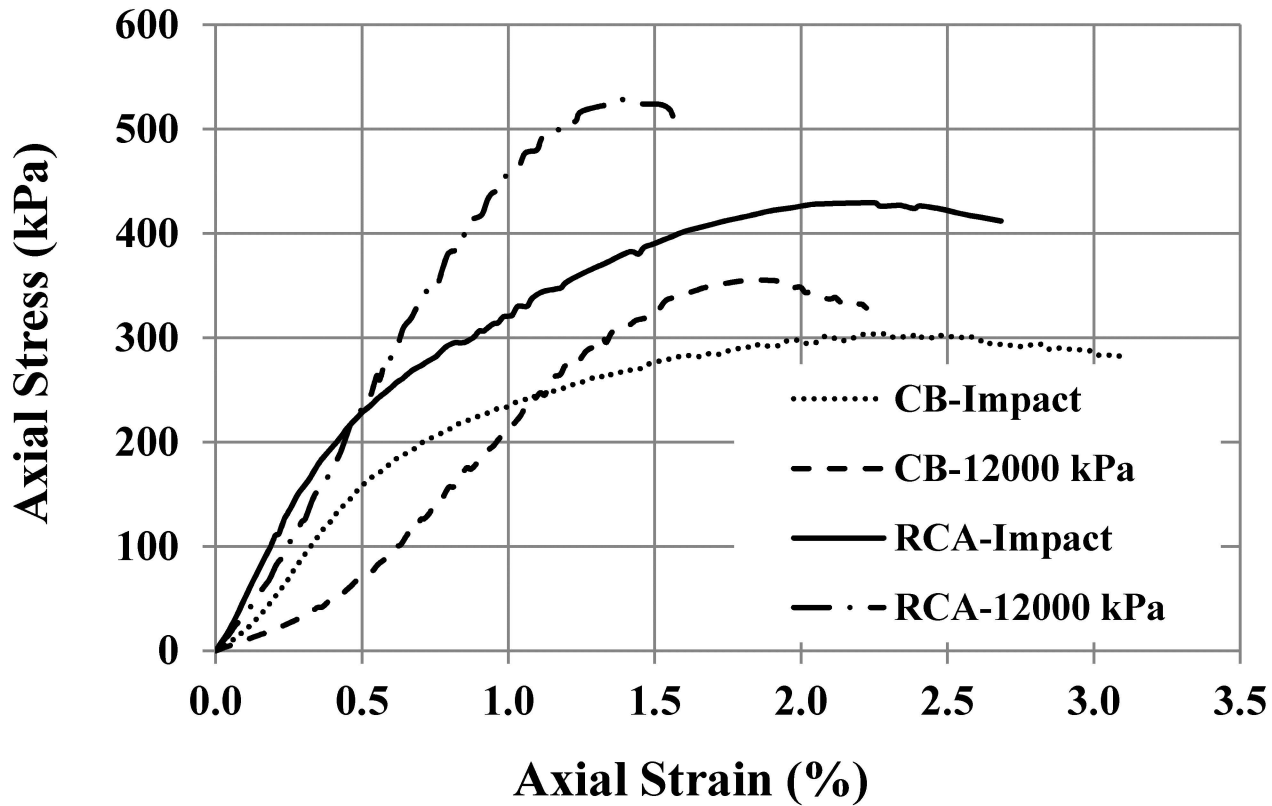


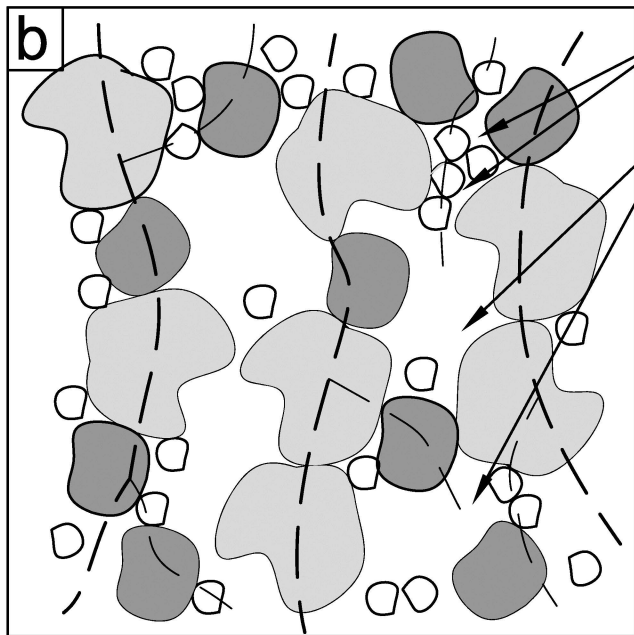
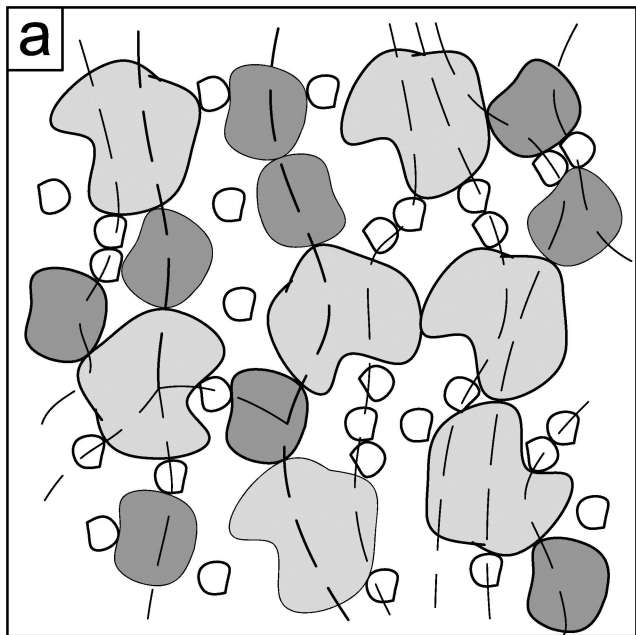












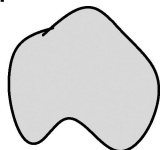
Higher Local Density

Lower Local Density

— — Force Chain  
(Thicker Line = Greater Force)

In both frames:

7 @



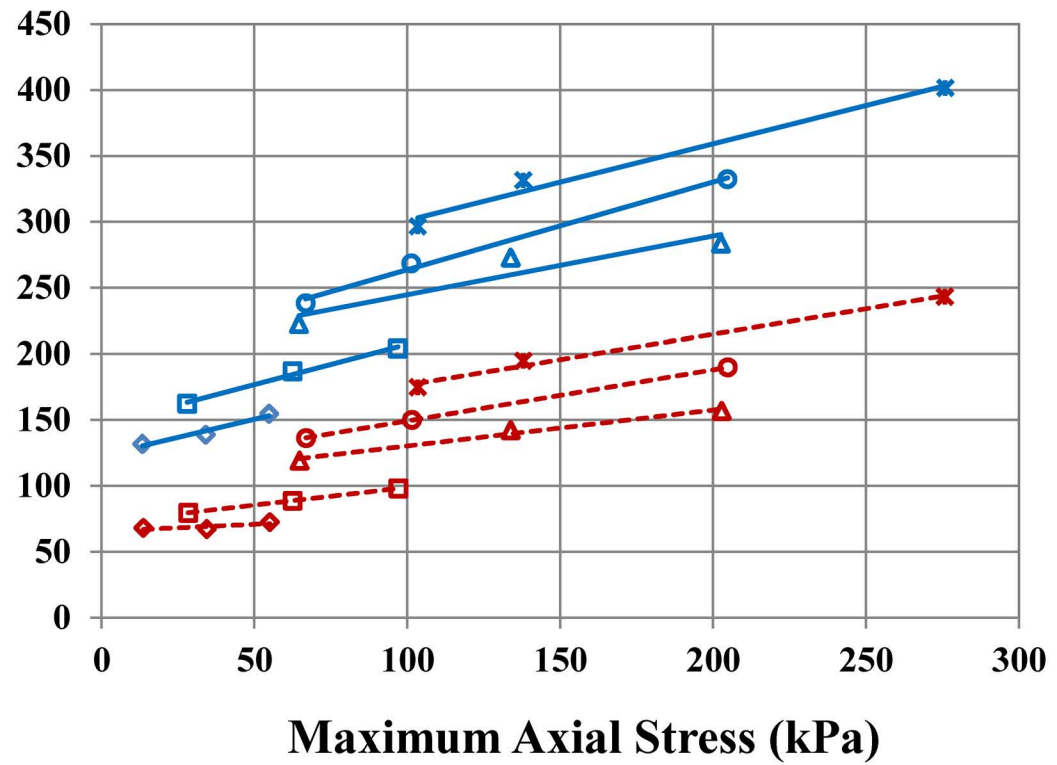
9 @



27 @



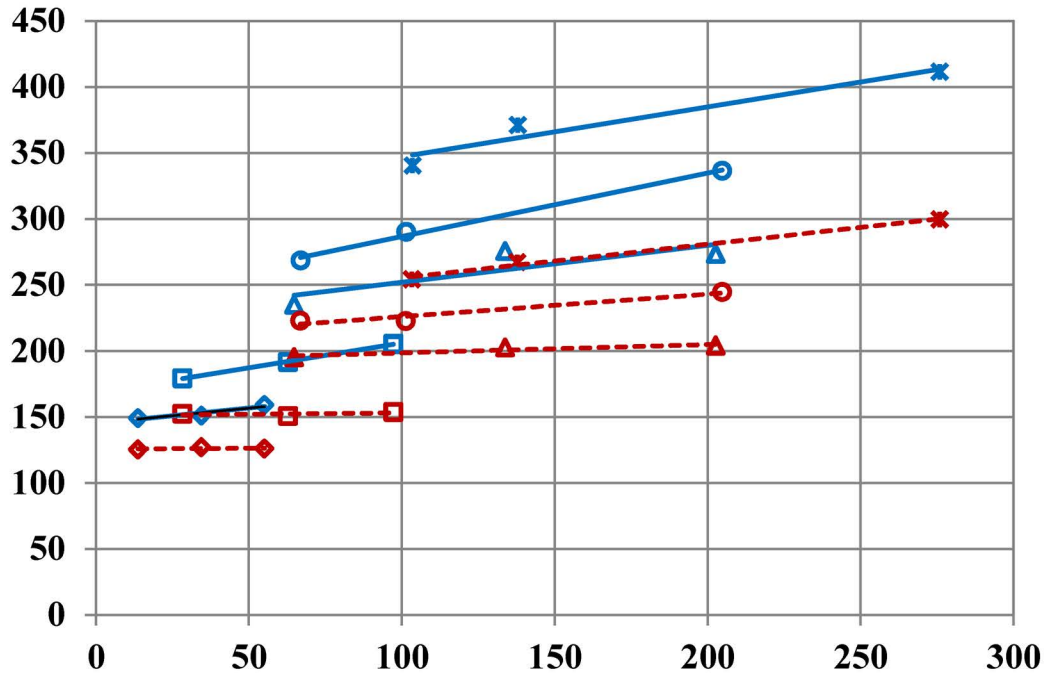
**Resilient Modulus (MPa)**



- ◆ CB-Impact ( $\sigma_c = 20.7$  kPa)
- CB-Impact ( $\sigma_c = 34.5$  kPa)
- △ CB-Impact ( $\sigma_c = 68.9$  kPa)
- CB-Impact ( $\sigma_c = 103.4$  kPa)
- × CB-Impact ( $\sigma_c = 137.9$  kPa)
- ◆ CB-12000 kPa ( $\sigma_c = 20.7$  kPa)
- CB-12000 kPa ( $\sigma_c = 34.5$  kPa)
- △ CB-12000 kPa ( $\sigma_c = 68.9$  kPa)
- CB-12000 kPa ( $\sigma_c = 103.4$  kPa)
- × CB-12000 kPa ( $\sigma_c = 137.9$  kPa)

**Maximum Axial Stress (kPa)**

**Resilient Modulus (MPa)**



**Maximum Axial Stress (kPa)**

- ◆— RCA-Impact ( $\sigma_c = 20.7$  kPa)
- RCA-Impact ( $\sigma_c = 34.5$  kPa)
- △— RCA-Impact ( $\sigma_c = 68.9$  kPa)
- RCA-Impact ( $\sigma_c = 103.4$  kPa)
- ×— RCA-Impact ( $\sigma_c = 137.9$  kPa)
- ◆- - RCA-12000 kPa ( $\sigma_c = 20.7$  kPa)
- - RCA-12000 kPa ( $\sigma_c = 34.5$  kPa)
- △- - RCA-12000 kPa ( $\sigma_c = 68.9$  kPa)
- - RCA-12000 kPa ( $\sigma_c = 103.4$  kPa)
- ×- - RCA-12000 kPa ( $\sigma_c = 137.9$  kPa)

